Journal of Stationarity (ISSN 2159-0648); Volume 1, No. 2; July 2011

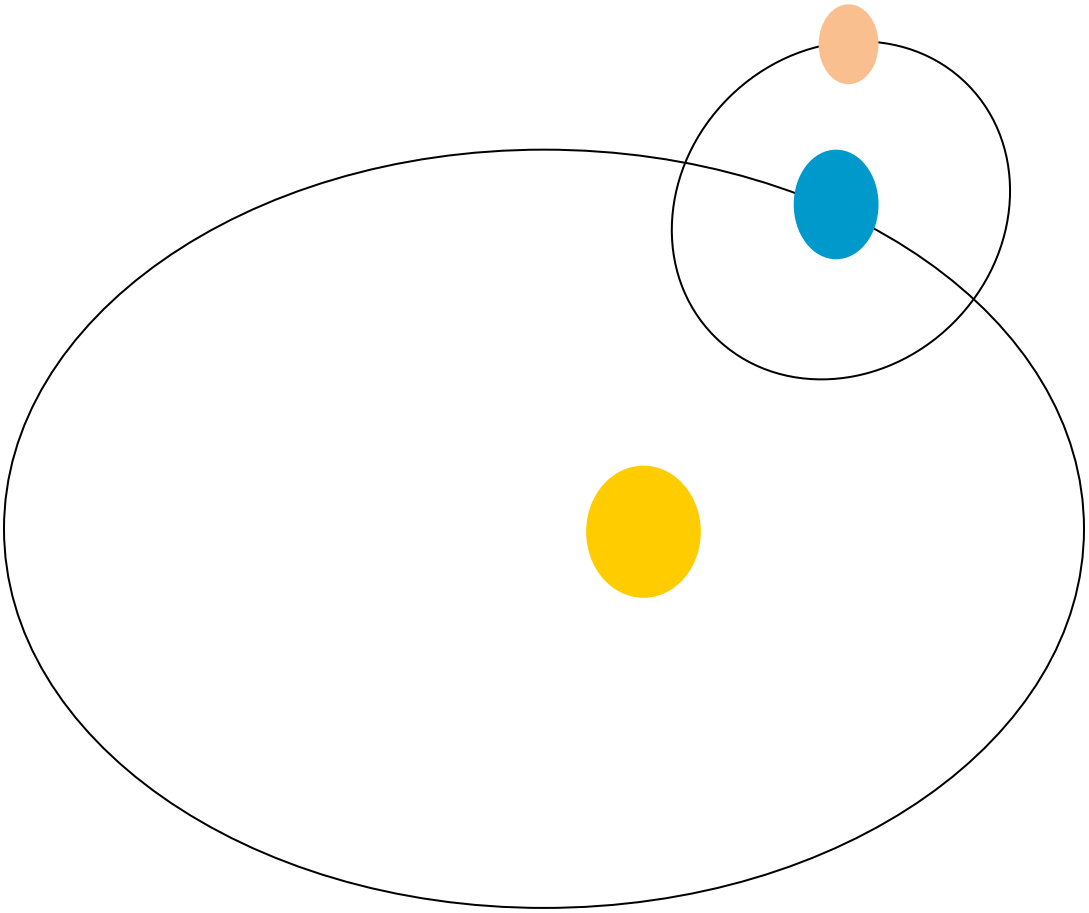

New Frontiers of Research towards the Predictability of Hydrological Variability, Earthquakes, and other Geophysical Processes

Messele Zewdie Ejeta (March 12, 2011)

In the afternoon of March 27, 1964, the second largest ever recorded earthquake hit Alaska, according to the National Oceanic and Atmospheric Administration (NOAA.) It generated tsunamis, which were recorded throughout the Pacific. It was the most disastrous to hit the West Coast of the U.S. and British Columbia, Canada.

In the aftermath of this disaster, the West Coast & Alaska Tsunami Warning System (WC&ATWS) was established to respond to the need for timely and effective tsunami warnings and earthquake information for Alaska and the northern Pacific (Sokolowski, 2011.)

Nearly 47 years later, in the afternoon of March 11, 2011, one of the largest ever recorded earthquakes hit Japan and generated tsunami waves that reached the coasts of Hawaii and the West Coast of the U.S.

A recent observation from my ongoing research to address uncertainties involved in the study of the impact of climate change on California's water projects suggests that geophysical processes including multidecadal hydrological variability and earthquakes may be predictable by using the transient positions of the moon around the earth and the moon and earth around the sun (Ejeta, 2011a, b.)

These movements can be gauged using solar eclipse trajectories (SETs) as proxies. SETs are based on Saros series and cycles, which have been established by the National Aeronautics and Space Administration (NASA.) My analysis using these proxies shows that two water years that have similar SETs tend to have similar hydrological conditions on earth (Ejeta, 2011b.) Similar SETs indicate that the transient movements of the moon around the earth are at similar distances from the earth at the same time of the given water years. A water year runs from the beginning of October of the previous calendar year through the end of September of the current calendar year.

Using letter codes of T, A, H, and P for Total, Annular, Hybrid, and Partial solar eclipse types and numeric orders for the calendar month in which the eclipse occurred, specific SETs can be established for any given water year. Thus, P1 means a partial solar eclipse event in January and P1-P6 means a trajectory of partial eclipses in January and June of the given year.

To gage the oncoming inertia of the movement of the moon around the earth and the moon and earth around the sun to a given water year, the solar eclipse trajectory of the previous water year may be added to establish a more robust longer SET.

Using this analysis approach, we find that water years 1964 and 2011 have similar SETs of A1-T7-P1-P6-P7. The specific Saros series, eclipse type, and eclipse magnitude data for these SETs are given in Table 1; a list of SETs for the 1903 to 2020 period is posted at http://www.jostationarity.com/VOL1/SETData.htm (Ejeta, 2011c) and provided in the next section.

Obviously, both water years 1964 and 2011 have similar solar eclipse trajectory characteristics. Therefore, this observation appears to suggest that there is an association between the similarities of cyclic SETs and geophysical processes on earth.

Table 1. Comparison of the 1964 and 2011 SETs and their characteristics (NASA, 2011)

Characteristics of 1964 SET (A1-T6-P1-P6-P7)				Characteristics of 2011 SET (A1-T6-P1-P6-P7)			
Date	Eclipse type	Saros Series	Eclipse magnitude	Date	Eclipse type	Saros Series	Eclipse magnitude
Jan. 25, 1963	Annular	140	0.995	Jan. 15, 2010	Annular	141	0.919
Jul. 20, 1963	Total	145	1.022	Jul. 11, 2010	Total	146	1.058
Jan. 14, 1964	Partial	150	0.559	Jan. 04, 2011	Partial	151	0.858
Jun. 10, 1964	Partial	117	0.754	Jun. 01, 2011	Partial	118	0.601
Jul. 9, 1964	Partial	155	0.322	Jul. 01, 2011	Partial	156	0.097

Various other natural events can be associated with the alignments or close alignments of the earth, moon, and sun. For example, on a sunny day on June 3, 2004, the Jones Tract in the Sacramento and San Joaquin River Delta near San Francisco, California, failed due to a higher than normal tide.

About a month earlier, on May 4, 2004, there was a Total lunar eclipse of Saros Series 131. It is plausible to theorize that if this levee's failure was due to an unusual tide during this lunar eclipse, it should have occurred on May 4, 2004, instead of nearly a month, or one lunar cycle later. However, the possibility that the high tide when the moon rotated back to a close location to the eclipse position hit a weak spot, or that it was already weakened enough because of previous high tides and gave in during the subsequent high tide, cannot be ruled out.

As another example, on a full moon day on December 26, 2004, an oceanic earthquake close to the coast of Sumatra triggered the Christmas Tsunami, which

indicates the influence of lunisolar forces (Gackstatter, 2007.) Half a synodic month later, on January 10, 2005, which was in a new moon phase, the first extreme proxigean spring tide and the first extreme lunisolar forces in the new millennium occurred (Gackstatter, 2007.) About two lunar cycles before the Christmas Tsunami, on October 28, 2004, there was a Total lunar eclipse of Saros series 136 (NASA, 2011.)

Newton's law of universal gravitation as it relates to tidal dynamics, which in turn may affect geophysical processes on earth, has been put forward as an area of focus in this further research. Gackstatter (2007) indicates that when the moon is full or new, the gravitational pull of the moon and sun are combined and result in spring tides. According to his insight, high spring tides occur when the moon is close to the earth on its elliptical path because the tide-raising force varies inversely as the third power of the lunar distance.

The focus herein and in Ejeta (2011a) surrounds the alignments of the earth, moon, and sun as recorded by solar and lunar eclipse events. When these alignments occur, the combined distance between these three celestial objects is the smallest, which translates to pronounced gravitational pull on the earth tides, according to Newton's law of universal gravitation.

While the physics behind the association of SETs and geophysical processes on earth is a subject of further investigation, the body of evidences of the associations is building up strongly.

References

Ejeta, M. Z. (2011a), Observed Association between Historical Major Earthquakes and Lunisolar Alignments, Proceedings of the American Society of Civil Engineers World Environmental and Water Resources Congress, Palm Springs, CA, May 22-26, 2011.

Ejeta, M. Z. (2011b), Transient Lunisolar Positions as Predictors of Earth's Hydrological Variability, Proceedings of the American Society of Civil Engineers World Environmental and Water Resources Congress, Palm Springs, CA, May 22-26, 2011.

Ejeta, M. Z. (2011c), Solar Eclipse Trajectories (SETs) for the 20th Century and First Two Decades of the 21st Century, Journal of Stationarity (in progress,) 2011.

Gackstatter, F. (2007), Lunisolar Effect on Spring Tides, Earthquakes, and Tsunamis, Journal of Coastal Research, 23(2), 528-530.

NASA (2011), NASA Eclipse Web Site, http://eclipse.gsfc.nasa.gov/eclipse.html, accessed 03/12/2011.

Sokolowski, T. J. (2011), The Great Alaskan Earthquake & Tsunami of 1964, http://wcatwc.arh.noaa.gov/64quake.htm, accessed 03/12/2011.

Solar Eclipse Trajectories (SETs) for the 20th Century and First Two Decades of the 21st Century

Messele Zewdie Ejeta

Each SET in the following table is a record of historical and projected trajectories of solar eclipse events for two consecutive water years. A water year runs from October 1st of the previous calendar year to September 30th of the current calendar year.

According to the National Aeronautics and Space Administration (NASA, 2011,) there are four types of solar eclipse events: Total (T,) Annular (A,) Hybrid (H,) and Partial (P.)

In the SET, a month in which a particular solar eclipse event occurred is denoted by a number; 1 for January, 2 for February, …, and 12 for December. Thus, an A1 designates an Annular solar eclipse event in January.

An A1-T7-P1-P6-P7 SET designates a trajectory of Annular and Total solar eclipse events in January and July of the previous year, respectively, and Partial solar eclipse events in January, June, and July of the current year. It is assumed that two SETs that are similar indicate similar movement of the moon around the earth and the earth and moon around the sun between the first and last events in the SET.

Note that both 1964 and 2011 have similar SETs. In 1964, one of the largest recorded earthquakes occurred in Alaska and in 2011, another large earthquake occurred in Japan. Two other years with similar SETs are 1946 and 1982. In 1946, another earthquake also occurred in Japan and in 1982 in Yemen.

Emerging studies (Ejeta, 2011) show that, on average, the gap between historically recorded major earthquakes (Richter Magnitude scale ≥ 7.0) and solar eclipse events is only a few days. These studies also show that when the moon is at the same distance from the earth at the same time of year, similar hydrological conditions tend to occur on earth.

Given these mounting evidences, it appears imperative to exert concerted efforts around the world towards the predictability of earthquakes and other geophysical processes. The similarity of hydrological conditions for two water years with similar SETs can be studied using historical precipitation data of the two years. NASA's data shows projected solar and lunar eclipse events out to the end of the 21st century and can be used to complete the projected SETs.

Table. Solar Eclipse Trajectories (SETs) for the 20th century and first two decades of the 21st century

Water Year	*Solar Eclipse Trajectory (SET)*	*Water Year*	*Solar Eclipse Trajectory (SET)*	*Water Year*	*Solar Eclipse Trajectory (SET)*
1903	A11-P4-P5-P10-A3-T9	1943	P3-P8-P9-T2-A8	1983	P1-P6-P7-P12-T6
1904	P10-A3-T9-A3-T9	1944	T2-A8-T1-A7	1984	P12-T6-A12-A5
1905	A3-T9-A3-T8	1945	T1-A7-A1-T7	1985	A12-A5-T11-P5
1906	T9-A3-T8-P2-P7-P8	1946	A1-T7-P1-P5-P6	1986	T11-P5-T11-P4
1907	P2-P7-P8-T1-A7	1947	P1-P5-P6-P11-T5	1987	T11-P4-H10-H3-A9
1908	T1-A7-T1-A6	1948	P11-T5-A11-A5	1988	H10-H3-A9-T3-A9
1909	T1-A6-H12-H6	1949	A11-A5-T11-P4	1989	T3-A9-P3-P8
1910	H12-H6-P12-T5	1950	T11-P4-P10-A3-T9	1990	P3-P8-A1-T7
1911	P12-T5-P11-T4	1951	P10-A3-T9-A3-A9	1991	A1-T7-A1-T7
1912	P11-T4-A10-H4	1952	A3-A9-T2-A8	1992	A1-T7-A1-T6
1913	A10-H4-T10-P4-P8-P9	1953	T2-A8-P2-P7-P8	1993	A1-T6-P12-P5
1914	T10-P4-P8-P9-A2-T8	1954	P2-P7-P8-A1-T6	1994	P12-P5-P11-A5
1915	A2-T8-A2-A8	1955	A1-T6-A12-T6	1995	P11-A5-T11-A4
1916	A2-A8-T2-A7	1956	A12-T6-A12-T6	1996	T11-A4-T10-P4
1917	T2-A7-P12-P1-P6-P7	1957	A12-T6-P12-A4	1997	T10-P4-P10-T3-P9
1918	P12-P1-P6-P7-A12-T6	1958	P12-A4-T10-A4	1998	P10-T3-P9-T2-A8
1919	A12-T6-A12-T5	1959	T10-A4-T10-A4	1999	T2-A8-A2-T8
1920	A12-T5-A11-P5	1960	T10-A4-T10-P3-P9	2000	A2-T8-P2-P7-P7
1921	A11-P5-P11-A4	1961	T10-P3-P9-T2-A8	2001	P2-P7-P7-P12-T6
1922	P11-A4-T10-A3-T9	1962	T2-A8-T2-A7	2002	P12-T6-A12-A6
1923	T10-A3-T9-A3-T9	1963	T2-A7-A1-T7	2003	A12-A6-T12-A5
1924	A3-T9-P3-P7-P8	1964	A1-T7-P1-P6-P7	2004	T12-A5-T11-P4
1925	P3-P7-P8-T1-A7	1965	P1-P6-P7-P12-T5	2005	T11-P4-P10-H4
1926	T1-A7-T1-A7	1966	P12-T5-A11-A5	2006	P10-H4-A10-T3-A9
1927	T1-A7-A1-T6	1967	A11-A5-T11-P5	2007	A10-T3-A9-P3-P9
1928	A1-T6-P12-T5-P6	1968	T11-P5-T11-P3-T9	2008	P3-P9-A2-T8
1929	P12-T5-P6-P11-T5	1969	T11-P3-T9-A3-A9	2009	A2-T8-A1-T7
1930	P11-T5-A11-H4	1970	A3-A9-T3-A8	2010	A1-T7-A1-T7
1931	A11-H4-T10-P4-P9	1971	T3-A8-P2-P7-P8	2011	A1-T7-P1-P6-P7
1932	T10-P4-P9-P10-A3-T8	1972	P2-P7-P8-A1-T7	2012	P1-P6-P7-P11-A5
1933	P10-A3-T8-A2-A8	1973	A1-T7-A1-T6	2013	P11-A5-T11-A5
1934	A2-A8-T2-A8	1974	A1-T6-A12-T6	2014	T11-A5-H11-A4
1935	T2-A8-P1-P2-P6-P7	1975	A12-T6-P12-P5	2015	H11-A4-P10-T3-P9
1936	P1-P2-P6-P7-A12-T6	1976	P12-P5-P11-A4	2016	P10-T3-P9-T3-A9
1937	A12-T6-A12-T6	1977	P11-A4-T10-A4	2017	T3-A9-A2-T8
1938	A12-T6-A12-T5	1978	T10-A4-T10-P4	2018	A2-T8-P2-P7-P8
1939	A12-T5-P11-A4	1979	T10-P4-P10-T2-A8	2019	P2-P7-P8-P1-T7
1940	P11-A4-T10-A4	1980	P10-T2-A8-T2-A8	2020	P1-T7-A12-A6
1941	T10-A4-T10-A3-T9	1981	T2-A8-A2-T7		
1942	T10-A3-T9-P3-P8-P9	1982	A2-T7-P1-P6-P7		

Observed Relationships among California's Record Short Droughts, Changes in the Phases of the Pacific Decadal Oscillation, and the Pacific Ocean's Cyclic Tide Level Peak Changes

Messele Zewdie Ejeta

Abstract

Based on an analysis of over a century of full natural flow data of California's eight major rivers, a strong relationship is observed between two short droughts on record and the two known Pacific Decadal Oscillation (PDO) shifts from the cool phase to the warm phase. The two short droughts on record, measured by the amount of full natural flows, occurred in water years 1924 and 1977 whereas the two known PDO cycle shifts since 1891 from the cool phase to the warm phase occurred with the ending of cool PDO phases in 1924 and 1976. In general, the full natural flows of these rivers during these two years were less than 25% of their corresponding long-term averages, which is considered herein as a drought condition. In addition, cyclic long-term increasing and decreasing trends of the Pacific Ocean's average tide level peaks as measured at the Golden Gate Bridge near San Francisco, California, appear to envelope the PDO phases. Such strong relationships between record short droughts and the PDO phase change timing as well as between PDO cycles and trends in tide level changes avail us an opportunity to further investigate if such strong relationships point to distinct forcing factors that caused and will likely cause them in the future. To the extent that the PDO can be predicted, as some emerging studies suggest, a foresight of its cycles and the changes in its phases may prove to be valuable for water resources planning and management in California.

Introduction

The western part of the United States in general and California in particular face both long-term and short-term recurring drought conditions, which have been defined using various approaches. Precipitation is generally used to define a hydrological drought. McCabe, et al. (2004) state that a drought condition in a given climatic region is considered to exist if annual precipitation was in the lowest quartile (25%) of the 100-year record. On the basis of this definition and for the purpose of this paper, a drought condition is considered to exist in a given river basin if the full natural flow of the basin falls in the lowest quartile of a Climatological standard normal flow record. The full natural flow, which is also called unimpaired runoff, is defined by the California Department of Water resources as the flow which represents the natural water production of a river basin, unaltered by upstream diversions, storage, or by

export or import of water to or from other watersheds (CA DWR, 2009.) The World Meteorological Organization (WMO) defines a Climatological standard normal as the average of climatological data computed for the following consecutive periods of 30 years (WMO, 1988.)

Historically, drought conditions are generally considered to have occurred in California during 1924, 1928-34, 1976 -77, and 1987-92. In water years 1924 and 1977, the full natural flow of seven of California's eight major rivers were the two lowest flows since record taking started at the beginning of the 20th century. For the eighth major river, the flows during those years are among the lowest three on record. In California, a water year spans from October 1st of the previous year to September 30th of the current year. This timeline avoids splitting the Southern Hemisphere summer wet season, or equivalently, the Northern Hemisphere winter wet season (Loewe and Radok, 1948.) Both localized and statewide drought emergencies have been declared between 2007 and 2009 (Office of the Governor, 2009.) Rainfall records of 2007 and 2008 were used among other indicators in the declaration of the statewide drought emergency in 2009. The economic consequences of these droughts have been enormous. A reasonable foresight of the state of the water supply of a given region a few years in advance will provide invaluable information in curbing the economic, social, and environmental consequences of a future drought.

Despite the importance of weather and climate variables as crucial for the planning and management of many real world problems, predicting them with reasonable accuracy, both spatially and temporally, have long been challenges. In addition, bridging the gap between the spatial and temporal scales of weather and climate is a significant challenge facing the atmospheric community (Cassou, 2008.)

Observed physical processes such as the solar climatic cycles (Willett, 1974), El Niño Southern Oscillation (ENSO, Trenberth and Shea, 1987,) Madden-Julian Oscillation (MJO, Madden and Julian, 1994,) Atlantic Multidecadal Oscillation (AMO, Goldenberg, et al., 2001,) Pacific Decadal Oscillation (PDO, Mantua and Hare, 2002,) and North Atlantic Oscillation (NAO, Hurrell, et al., 2003) are factors that explain some variations in weather and climate variables. The fundamental causes of most of these observed physical processes, their persistence, rates of change, and short-term and long-term effects on our environment are yet to be fully understood, characterized, and explained.

Various research efforts have shown in a piecemeal approach some of the uses of these observed processes for weather and climate prediction. Willett (1974) noted the awareness of solar-climatic relationships and the prevailing attitude at that time that

despite such relationships being real, they were considered too small to be of practical prognostic value. His study defined and characterized three sunspot cycles, which include: 1) Basic 11-year cycle (varies from 9 to 14 years), 2) Double sunspot cycle (varies from 20 to 26 years), and 3) Secular cycle (alternately 100 and 80 years.) According to this study, the last secular cycle of 100 years extended from the sunspot minimum of 1878 to that of 1977-1978. In retrospect, this study provided a crucial projected piece of information at that time that nearly coincided with the PDO phase shift between 1976 and 1977 and the worst drought on record in California since 1901, as measured by the full natural flows of its major rivers.

The PDO, which is one of the variables this paper focuses on, is a long-lived El Niño-like pattern of Pacific climate variability, including sea surface temperature, sea level pressure, and sea surface wind stress. The term was coined in 1996 by fisheries scientist Steven Hare while researching connections between Alaska salmon production cycles and Pacific climate. In the 20th century, PDO phases, characterized as cool and warm, persisted from 20 to 30 years. Cool PDO regimes prevailed from 1890-1924 and again from 1947-76. Warm PDO regimes dominated from 1925-46 and from 1977 through (at least) the mid-1990's (University of Washington, 2009.) Thus, the time about 1924 and 1976 are the two years in the 20th century when the PDO phase shift from the cool phase to warm phase occurred.

Other studies after the pioneering work of Willett (1974) have shown that during the 1976-77 winter season, there was an abrupt shift in the climate state of the North Pacific Ocean (Ebbesmeyer, et al., 1991, Graham, 1994.) Other later studies have focused on the variance of the frequency of droughts in the United States and attributed it partly to observed physical processes. McCabe, et al. (2004) found that about 52% of the spatial and temporal variance in multidecadal drought frequency over the conterminous United States is attributable to the PDO and AMO. While Willett's (1974) projection of secular cycle sunspot minimum practically coincided with a record drought occurrence in California, McCabe, et al.'s (2004) study points to the variance of drought frequencies. The coincidence of the PDO shift from the cool to warm phase in 1976 with the 1976-77 drought provides a new piece of information for the study of drought occurrences.

An important question may be raised here, which is whether the coincidental occurrences of the PDO phase shift, sunspot minimum of the secular cycle, and record drought in California about 1976-77 point to underlying fundamental physical processes that are yet to be fully understood. While Jones et al. (1986) point to observed occurrences of gradual drifts, a series of long-term swings, and abrupt

changes in climate, other studies have argued that we have little understanding of the physical processes behind these occurrences (Karl, 1988; Wunsch, 1992). Miller, et al. (1994) note the paramount importance of the study of various natural climate variations to better understand the effect of Green House Gas (GHG) emissions on climate. Natural variability has traditionally rendered both practitioners and trainers the sense of stationarity, which is the idea that natural systems fluctuate within an unchanging envelope of variability (Milly, et al., 2008.) Milly, et al. (2008) also argue that stationarity is dead because of the effect of elevated GHG emissions to the atmosphere in recent times. However, the currently widely believed dead stationarity may be unlikely to erase natural variability altogether; it will most likely continue to live as the undercurrent beneath dead stationarity. Thus, a better understanding of the causes of the physical processes that cause natural variability and their effects on weather and climate remains important in reducing uncertainties in climate change modeling processes for water resources planning, among others. McCabe, et al. (2007) suggest that understanding the sources of decadal to multi-decadal hydroclimatic variability will help improve water resources planning over the long-term.

Observed data has become crucial in understanding the causes of natural variability (Meehl, et al. 2009.) In fact, there are emerging studies that hypothesize that at least some of these variables may have deterministic mechanisms. Power and Colman (2006) suggest that PDO pattern may have deterministic mechanisms that are separate from ENSO and thus may be predictable beyond the ENSO time scale. Wu, et al. (2009) presented an empirical model to predict the East Asian Summer Monsoon strength using the El Niño Southern Oscillation (ENSO) and the spring North Atlantic Oscillation (NAO.)

Traditionally, the realizations of climate variables have been considered pseudo-random events and analyzed using statistical techniques (Mann, et al., 2009.) However, the coincidences of the sunspot minimum of the secular solar cycle, PDO phase shift, and short drought in California appear to be far from random. Observed cyclic long-term increasing and decreasing trends of the Pacific Ocean's tide level peaks, as measured at the Golden Gate Bridge near San Francisco, California, will be shown later in this paper to envelope the PDO phases. In addition, the tide level peak changes appear to show relationships between the magnitudes of these changes and record wet spells in California. These new observations add a new dimension to a continuing emergence of physical processes that relate to climate variables. The effort of this paper is thus to analyze and illustrate the observed relationships among these variables to establish a baseline for further investigation of a three-way relationship between full natural flows, PDO phases and shifts, and tide level peaking cycles and

trends. In effect, it points to a departure from statistical analysis of climate variables to focus on a deterministic approach, which is the basis for multidecadal predictability.

Relevance of California's Full Natural Flows in Its Water Project Operations

The operation of California's two major water projects, the State Water Project (SWP) and Central Valley Project (CVP), is based on the implementation of the California State Water Resources Control Board's (SWRCB) water right decision D1485 (passed in 1978) and Water Quality Control Plan (WQCP) decision D1641 (passed in 1995). Decision 1485 classified the water supply conditions of the Sacramento and San Joaquin valleys into five water year types using the full natural flows of four major rivers in each valley. These water year types are termed Wet, Above Normal, Below Normal, Dry, and Critical. In the Sacramento Valley, the full natural flows of the four rivers used for water year type classifications are the Sacramento River at Bend Bridge, Feather River at Oroville, Yuba River at Smartville, and American River at Folsom Dam. In the San Joaquin Valley, the full natural flows used are the Stanislaus River at New Melones Lake, Tuolumne River at New Don Pedro Reservoir, Merced River at McClure Lake, and San Joaquin River at Millerton Lake. Figure 1 shows these flow locations.

Even though the water supply conditions for the operation of the state's major water projects is clearly defined by the SWRCB, the implementation of the SWRCB's decisions in the actual operation of the projects is based on a limited prognostic capability. This is because of the prevailing limited skill in forecasting rainfall and runoff events for a long enough time. The trajectories of streamflows that have been produced through climate change modeling processes for different emission scenarios, represented by different General Circulation Models (GCMs,) disaggregated to regional scales using statistical techniques, run through coarse scale hydrologic models, and routed to specific streamflow locations are too uncertain to have bearings in availing any lead time for the operation of these water projects. Thus, the search for a strong prognostic capability in streamflows is driven by the desire to 1) curb the effect of extreme events of droughts and floods by having reasonable foresight of water supply conditions, and 2) reduce the uncertainties in streamflow data obtained from the processes of climate change modeling.

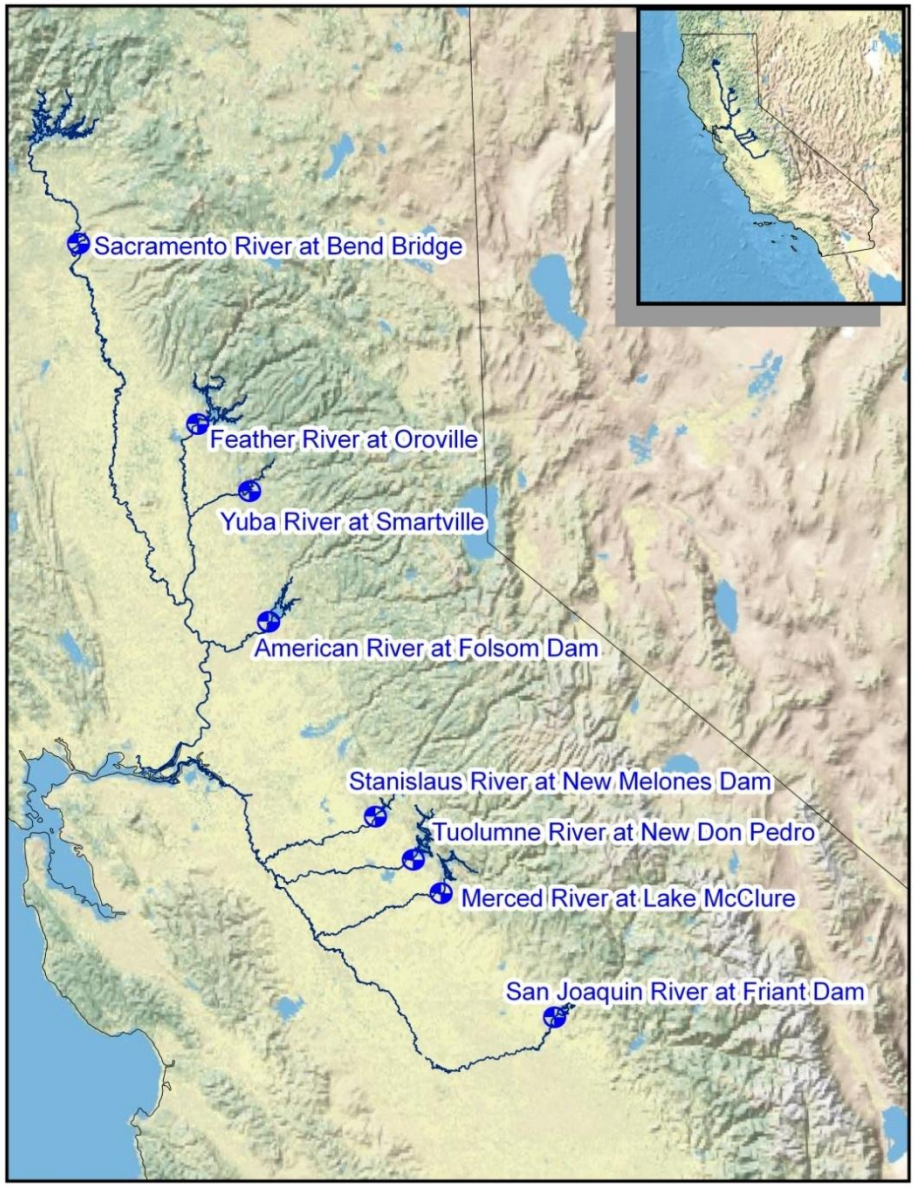

Figure 1. California's eight major rivers with over 100 years of estimated full natural flow data (Ejeta, et al. 2009)

Stationarity versus Natural Variability in Full Natural Flow

The traditional water resources project planning assumes that, on average, the variability of historical hydrological data for a given region can be used as a predictor of its future variability. Even though this stationarity in hydrological data is generally evident in over a century of observed full natural flows of California's major rivers

(Figure 2), so far, there have not been specifically defined physical processes that are known to be the cause of it. A closer look at the anomalies of a 30-year moving average of the water year flows of these major rivers shows a sinusoidal nature of the long-term full natural flows. A similar analysis of the PDO Index's anomalies also shows its sinusoidal nature. Figure 3 depicts these anomalies for the PDO Index and the Feather River flow at Oroville with a fourth degree polynomial function as a preliminary fit, which has R^2 value of about 0.90. A study of the two sets of anomalies shows a correlation of about 54%. Both graphs suggest that there may be forcing factors with their own periodicities that are at a play.

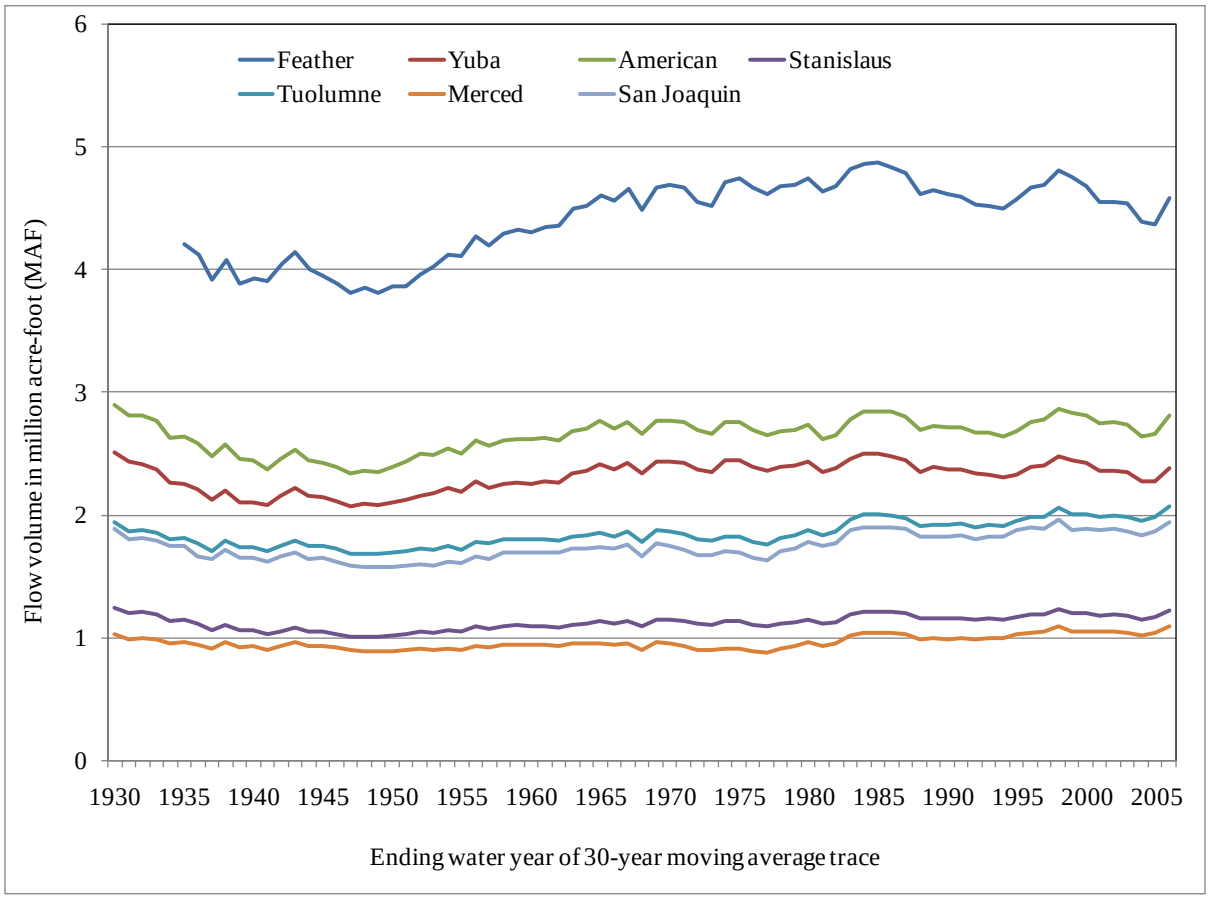

Figure 2. 30-year moving average trace of the full natural flows of California's major rivers

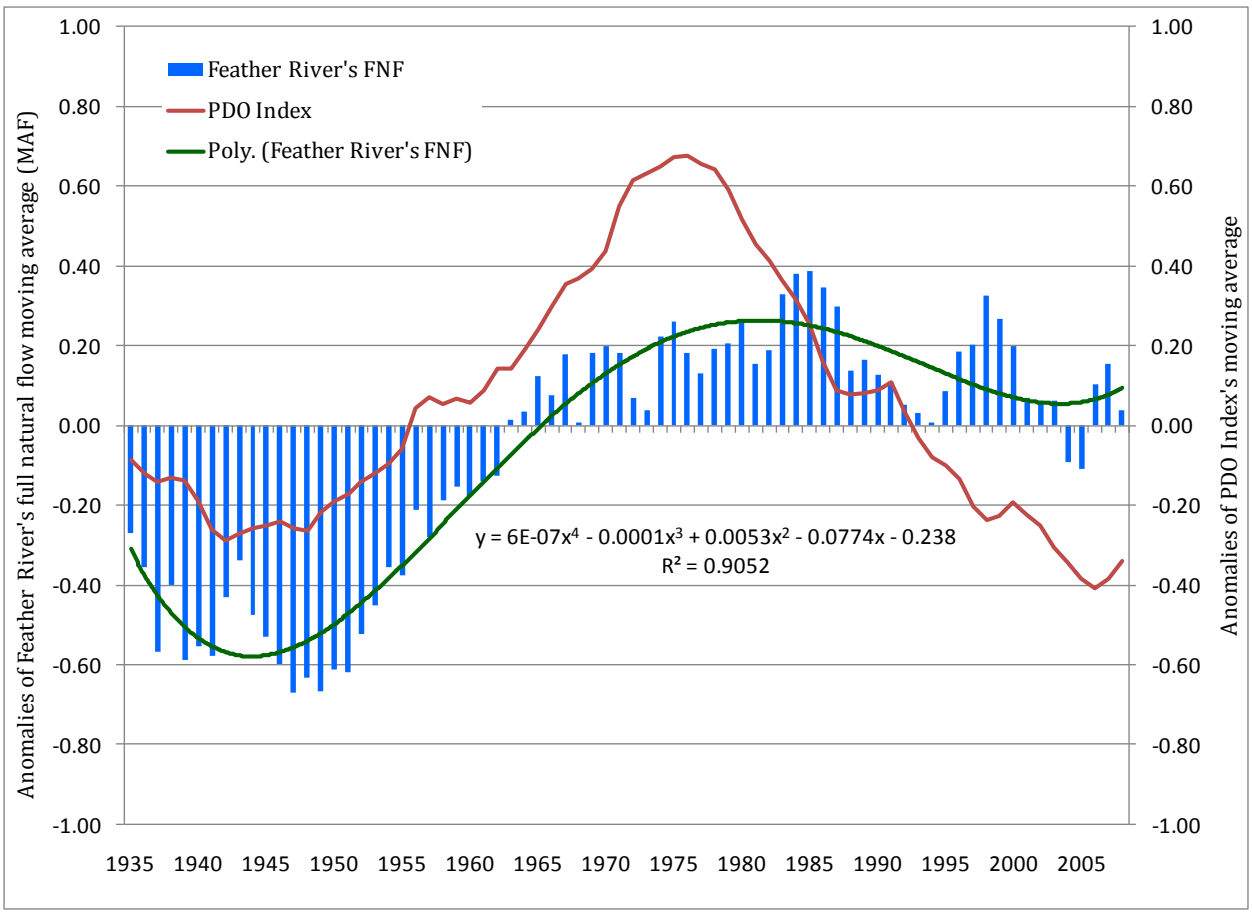

Figure 3. Anomalies of 30-year moving averages of: 1) full natural flow of Feather River at Oroville (blue bars, in million acre-foot, with 4th degree polynomial trend line fit, green line) and 2) the PDO Index (red line)

Long-term Trends in Annual Flows

An analysis of the Cumulative Standardized Departures (CSDs) of the full natural flows, which are normalized deviations of the individual water year data from the corresponding long-term mean, shows a discernible pattern around historically known droughts in California. These patterns are consistently similar in the data of all the eight rivers. Figure 4 is a sample illustration of the CSDs for the full natural flow of the Feather River at Oroville, California. This analysis shows that the CSDs started to have a generally declining slope starting about 1916 and ending around the end of the Dust Bowl around 1937. If this data could be considered as an indicator, the moisture deficit during the Dust Bowl may well have been set in motion by momentous deficiencies in rainfall that started to occur about 1916.

Between the end of the Dust Bowl and the short-term record drought of 1976-77 that was followed by the short-term wet-spell on record of 1983, the CSDs show relatively stable water productions by the rivers with moderate events to the extremes.

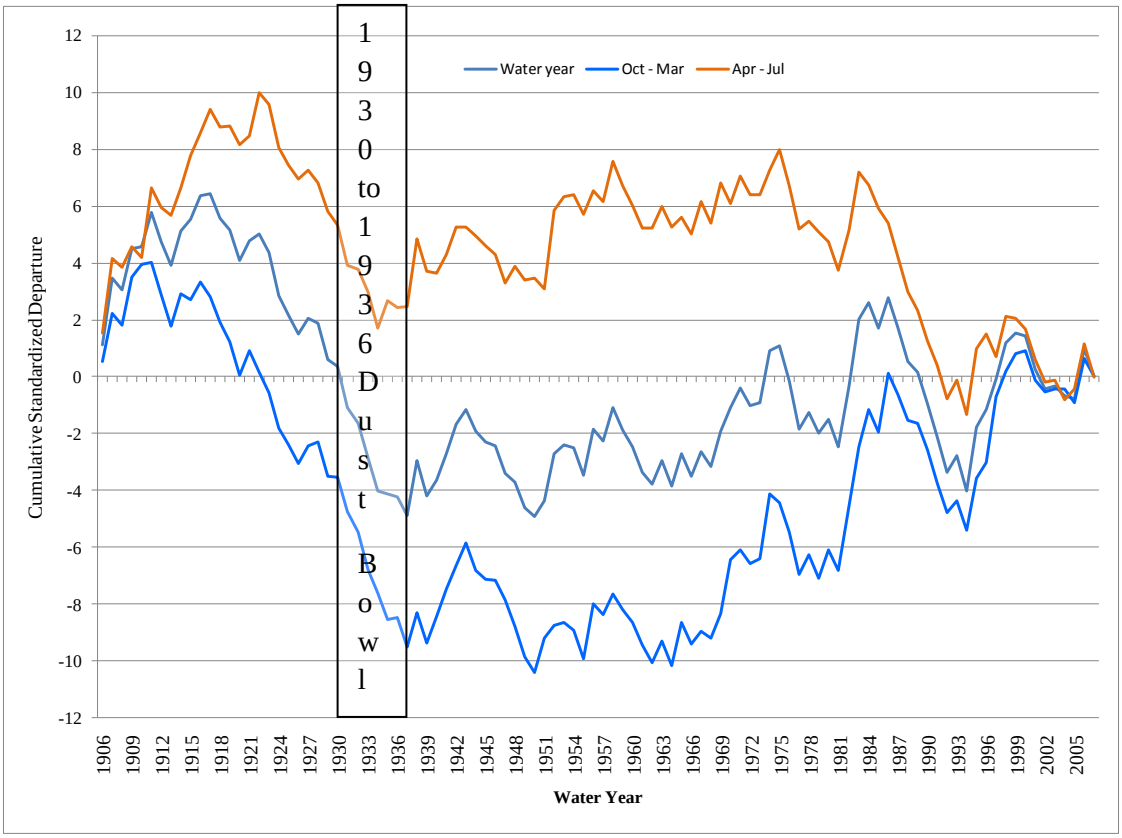

Figure 4. Cumulative Standardized Departures of Feather River full natural flow at Oroville

Observed Trends in Tide Level Peaks

The fluctuation since 1900 in historical tide levels at the Golden Gate Bridge near San Francisco, California, shows markedly high fluctuations between 1940-42 and 1983-84. During each of these two short intervals, the tide level fluctuates by about 0.6 and 0.8 feet, respectively, as shown in Figure 5. These markedly high tide level fluctuations coincide with the wet spells in California between 1941-43 and 1982-84, all wet water year types as measured by the Sacramento Valley water year type index. The highest tide level fluctuation on record between 1983-84 coincides with the 1983 wettest year on record in California. Between 1908-14 and 1942-83, there are generally increasing

trends of tide level peaks. For the remaining time segments during which data is available, there are generally decreasing trends of tide level peaks. The trends in the tide level troughs are not as apparent as the trends of the peaks.

Thus, it can be observed from the trends of the tide level peaks that there are cyclic long-term increasing and decreasing trends. Furthermore, allowing for a few transitional years, an increasing trend in tide level peaks (prior to 1914 and between 1942-83) is generally observed during cool PDO phases whereas a decreasing trend in tide level peaks (1914-42 and since 1984) is generally observed during warm PDO phases (see Figure 5.) The timing of the marked fluctuations suggests a possible correlation between these events and the 1946-47 and the 1976-77 phase shifts in the PDO cycles.

As ocean tides are caused by the gravitational pull by the Moon and Sun (Rahmstorf, 2002,) it is conceivable that the apparent cyclic trends in the tide level peaks and the lack of such trends in their troughs could be due to the relative positions of the ocean bodies, Moon, and Sun. The patterns are apparently evident in the pulling phase (rising tide level peaks) but not so in the receding phase (falling tide level peaks.) The universal law of gravity assumes the earth as a monolithic mass, instead of an integral mass with its various components that may have multiple centers of gravity, which could potentially shift marginally depending on the relative positions and movements of the Moon and Earth around the Sun. However, the fact that the pull of the ocean body by the Moon and Sun is observable in the tide levels suggests that there must be distinct centers of masses to which the universal law of gravity may be applicable. This thesis leads to revisiting the utility of point mass principle in applying Newton's universal law of gravity to the movement of the Moon and Earth relative to the Sun and its possible effect on the weather and climate of the Earth.

Discussions

The ability to have a reasonable forecast of water supply conditions due to natural forcing factors will have significant bearings on the operations of large water projects as well as in reducing the uncertainties involved in the processes of climate change modeling. The relationship between recorded full natural flows in California and the shift in the PDO from the cool phase to the warm phase appears to show an emerging evidence that point to natural processes that affect full natural flows, and hence rainfall, at least in the west coast United States. Furthermore, the relationship between the Pacific Ocean's tide level peaking trends and cycles, as observed at the Golden Gate Bridge near San Francisco, and the PDO phases and shifts is also likely to point to an emerging evidence for natural forcing factors that may have caused it.

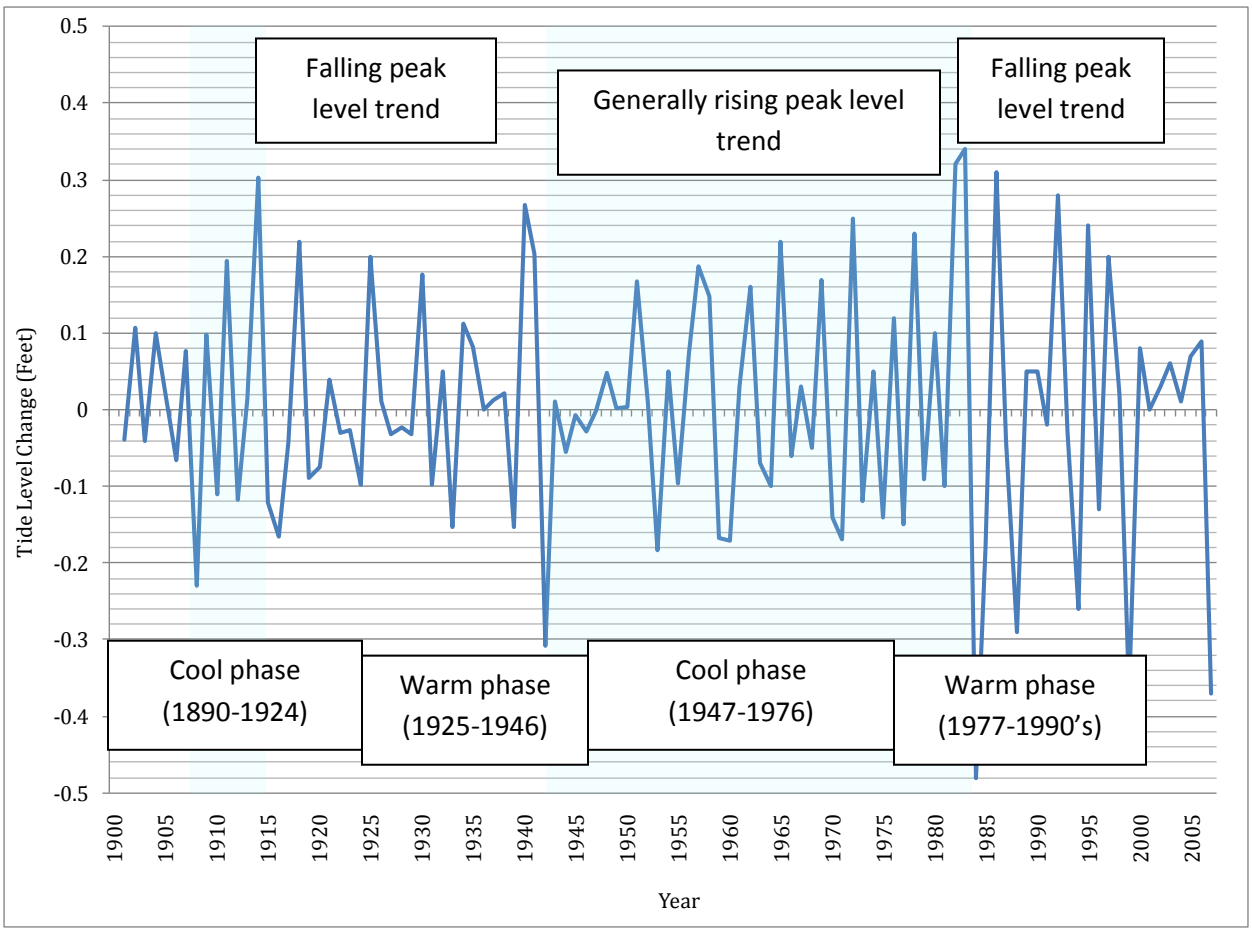

Figure 5. Mean tide level change at Golden Gate Bridge, San Francisco, California

In effect, these observed relationships may be useful to establish a baseline for further investigation of a three-way relationship between full natural flows, PDO phases and shifts, and tide level peaking trends and cycles. Moreover, the coincidence of the PDO shift between 1976 and 1977, the lowest full natural flow in California since records started to be taken at the turn of the 20th century, and the solar-climatic cycle change that had been projected to occur around 1977-78 appear to provide a fertile ground for further investigation about the physical processes behind these natural phenomena. These investigations are likely to lead to a better capability to predict rainfall and hence streamflows on a decadal to multi-decadal timescales.

The evidences presented herein can't be conclusive about all the forcing factors that cause the realizations of these observed relationships. However, it is conceivable that the pattern in the tide level peaking trends and cycles may be caused by the cyclic movements of the objects that are the drivers of the tide level fluctuations. It is also

conceivable that these cyclic movements have their own periodicities that can be characterized further, which is a subject of an ongoing investigation. In effect, this subject calls for the application of Astrohydrology, or the study of a possible correlation between astronomical trajectories of the Moon and Earth relative to the Sun and hydrological data on the ground on Earth. This concept is already built in our understanding of Earth's winter and summer seasons, which are caused by the trajectory of the Earth's movement around the Sun. The extension of this concept to include the trajectory of the Moon may bring the prediction of hydrology on a decadal to multi-decadal scales one step closer to our predictive capability of the winter and summer seasons of a year.

References

California Department of Water Resources (2009), California Data Exchange Center, Daily Full Natural Flows for December 2009, http://cdec.water.ca.gov/cgi-progs/stages/FNF (accessed December 24, 2009)

Cassou, C. (2008), Intraseasonal interaction between the Madden–Julian Oscillation and the North Atlantic Oscillation, *Nature*, 455, 523-527

Ebbesmeyer, C.C., D.R. Cayan, D.R. McLain, F.H. Nichols, D.H. Peterson and K.T. Redmond (1991), 1976 step in the Pacific climate: Forty environmental changes between 1968-75 and 1977-1984, *In Proc. 7th Annual Pacific Climate Workshop,* Calif. Dept. of Water Resources, Interagency Ecological Studies Program, Report 26.

Ejeta, M., T. Kadir, and J. Wang (2009), Analysis, Methodologies, and Evaluations, A Technical Memorandum Report

Francis, R. C., S. R. Hare, A. B. Hollowed, and W. S. Wooster (1998), Effects of Interdecadal Climate Variability on the Oceanic Ecosystems of the NE Pacific, *Fisheries Oceanography*, 7, 1-21

Goldenberg, S. B., C. W. Landsea, A. M. Mestas-Nuñez, and W. M. Gray (2001), The Recent Increase in Atlantic Hurricane Activity: Causes and Implications, *Science*, 293:5529, 474-479

Graham, N.E., 1994: Decadal scale variability in the 1970's and 1980's: Observations and model results. *Climate Dynamics,* 10*,* 60-70.

Hurrell, J. W., Y. Kushnir., G. Ottersen, and M. Visbeck, M. (2003), In *North Atlantic Oscillation: Climate Significance and Environmental Impact*, Eds. Hurrell, J. W., Kushnir, Y., Ottersen, G. & Visbeck, M., Geophysical Monograph, 134, 1–35

Jones, P.D., T.M.L. Wigley and P.B. Wright, (1986), Global temperature variations between 1861 and 1984, *Nature,* 322*,* 430-434.

Karl, T.R. (1988), Multi-year fluctuations of temperature and precipitation: the gray area of climate change. *Climatic Change,* 12*,* 179-197.

Loewe, F. and Radok, U. (1948), Variability and periodicity of meteorological elements in the Southern Hemisphere with particular reference to Australia, Canberra, Commonwealth of Australia

Madden, R. A. and P. R. Julian (1994), Observations of the 40–50 day tropical oscillation. *Monthly Weather Review,* 112, 1109–1123

Mann, M. E., J. D. Woodruff, J. P. Donnelly, and Z. Zhang (2009), Atlantic hurricanes and climate over the past 1,500 years, *Nature*, 460, 880-883

Mantua, N. J. and S. R. Hare (2002), The Pacific Decadal Oscillation, Journal of Oceanography, 58**,** 35–44.

McCabe, G. J., J. L. Betancourt, S. T. Gray, M. A. Palecki, H. G. Hidalgo (2007), Associations of multi-decadal sea-surface temperature variability with US drought, Science Direct Quaternary International, 188, 31-40

McCabe, G. J., M. A. Palecki, J. L. Betancourt (2004), Pacific and Atlantic Ocean influences on multidecadal drought frequency in the United States, PNAS 101, 4136-4141

Meehl, G. A., L. Goddard, J. Murphy, R. J. Stouffer, G. Boer, G. Danabasoglu, K. Dixon, M. A. Giogretta, A. M. Greene, E. Hawkins, G. Hegerl, D. Karoly, N. Keenlyside, M. Kimoto, B. Kirtman, A. Navarra, R. Pulwarty, D. Smith, D. Stammer, and T. Stockdale, Decadal prediction: can it be skillful?, American Meteorological Society, 1467-1485

Miller, A. L., D.R. Cayan, T.P. Barnett, N.E. Graham, and Josef M. Oberhuber (1994), The 1976-77 Climate shift of the Pacific Ocean, Oceanography, 7:1, 21-26

Milly, P. C. D., J. Betancourt, M. Falkenmark, R. M. Hirsch, Z. W. Kundzewicz, D. P. Lettenmaier, R. J. Stouffer (2008), Stationarity is dead: wither water management?, Science 319, 573-574.

Office of the Governor (2009), Gov. Schwarzenegger Takes Action to Address California's Water Shortage, http://gov.ca.gov/press-release/11556/ (accessed December 27, 2009)

Power, S. and R. Colman (2006), Multiyear predictability in a coupled general circulation model, *Climate Dynamics*, 26, 247-272

Rahmstorf, S. (2002), Ocean circulation and climate during the past 120,000 years, Nature, 419, 207-214

Trenberth, K. and D. J. Shea (1987), On the evolution of the Southern Oscillation, *Monthly Weather Review,* **115**, 3078–3096

Willett, H. (1974), Recent Statistical Evidence in Support of the Predictive Significance of Solar-Climatic Cycles, *Monthly Weather Review*, 102: 679-686

WMO (1988), General Meteorological Standards and Recommended Practices, Technical Regulations, Volume I, Basic Documents No. 2, WMO Publication No. 49, Geneva, Switzerland.

Wu, Z., B. Wang, J. Li, and F.-F. Jin (2009), An empirical seasonal prediction model of the east Asian summer monsoon using ENSO and NAO, J. Geophys. Res., 114

Wunsch, C. (1992), Decade-to-century changes in the ocean circulation, *Oceanography,* 5*,* 99-106

University of Washington (2009), The Pacific Decadal Oscillation (PDO), http://jisao.washington.edu/pdo/ (accessed November 30, 2009)

Temporal and Spatial Variations in Lunisolar Positions as Predictors of Hydrological Conditions on Earth

Messele Zewdie Ejeta

Abstract

An analysis of the hydrological conditions at Davis, California, using over a century of precipitation data with respect to the historical trajectories of the earth and moon relative to the sun, as recorded by solar eclipse events and their cyclic Saros series, shows a predictability of these hydrological conditions at the local level. Solar eclipse events that have the same Saros series, which have similar geometries in the earth-moon-sun vector field, are used as indicators for the position of the moon being at about the same node at the same time of year. The analysis indicates that two years that are separated by one or multiples of a Saros cycle of 18 years, 11 days, and 8 hours exhibit similar hydrological conditions at this location. The observed long-term association between these variables and the relative positions of these celestial objects is used to infer the predictability of hydrological conditions at the global scale. Since projected solar eclipse data out to the end of the 21st century is available from the National Aeronautics and Space Administration (NASA), the observed relationships may be used to predict decadal to multidecadal wet and dry spells in California as well as on a global scale. Further analysis of this momentous breakthrough in our understanding of earth's hydrology may bring the prediction of hydrological phenomena on earth one important step closer to our predictive capability of the winter and summer seasons of a year.

Introduction

The efforts of hydrologists to close earth's water balance by measuring where and in what quantities earth stores water and how water moves between those stores have been facing challenges for a long time (Lettenmaier and Famiglietti, 2006). Natural variability has traditionally rendered both practitioners and trainers the sense of stationarity, which is the idea that natural systems fluctuate within an unchanging envelope of variability (Milly, et al., 2008). The forcing factors that have been maintaining this intuitively understandable concept of natural variability have not been fully understood, characterized, and explained. Observed physical processes such as solar climatic cycles (Willett, 1974), El Niño Southern Oscillation (ENSO) (Trenberth and Shea, 1987), Madden-Julian Oscillation (MJO) (Madden and Julian, 1994), Atlantic Multidecadal Oscillation (AMO) (Goldenberg, et al., 2001), Pacific Decadal Oscillation (PDO) (Mantua and Hare, 2002), and North Atlantic Oscillation (NAO)

(Hurrell, et al., 2003) have been considered as factors that explain some variations in weather and climate. Some of these factors have been found to partly explain the variance of the frequency of droughts in the United States. McCabe, et al. (2004) found that about 52% of the spatial and temporal variance in multidecadal drought frequency over the conterminous United States is attributable to the PDO and AMO. Wu, et al. (2009) presented an empirical model to predict the East Asian Summer Monsoon strength using the ENSO and spring NAO. There are currently ongoing studies using General Circulation Models to predict decadal to multidecadal variations, yet some unresolved questions remain regarding not only how to conduct such predictions, but also regarding the quality and usefulness of the results (Meehl, et al., 2009).

Ongoing investigations have focused on reducing uncertainties surrounding general circulation modeling processes by closely analyzing various historical datasets, which have been acknowledged to be crucial to deal with uncertainties (Meehl, et al., 2009). One of the historical data sets being analyzed is that of ocean tide changes, which are known to be caused by the gravitational pull by the moon and sun (Rahmstorf, 2002). An analysis of over a century of tide level fluctuations of the Pacific Ocean, as measured at the Golden Gate Bridge, near San Francisco, California, shows multidecadal cyclic tide level peak trends. Thus, it is conceivable that such trends could be due to the relative positions of the ocean bodies, moon, and sun, and possibly other celestial objects. In fact, efforts have been made to establish links between transient tidal dynamics and the phases of the moon (Wood, 2001).

Newton's law of universal gravitation assumes the earth as a monolithic mass, instead of an integral mass with its various components that may have multiple centers of gravity, which could potentially shift marginally depending on the relative positions and movements of the moon around the earth and the moon and the earth around the sun. The fact that the pull of the ocean body by the moon and sun is observable in the form of tide levels suggests that there must be distinct centers of masses of water bodies on earth to which the law of universal gravitation may be applicable. This thesis leads to revisiting the utility of point mass principle in applying this law to the movements of the moon and earth relative to the sun and their possible effects on the weather and climate of earth.

Thus, the analysis presented herein hinges on the alignments of the earth, moon, and sun, as demonstrated by the Annular, Total, and Hybrid Solar Eclipses (ASE, TSE, and HSE) to characterize hydrological conditions on earth using long-term precipitation data at Davis, California. Four season, or two calendar year, solar eclipse

trajectories (SETs) for the various transient episodes of historical eclipses over the four seasons of a water year are designated and relationships are established between these events and the wet and dry spells observed on earth using this long-term precipitation data. Solar eclipse episodes that have the closest characteristics to a known SET are designated as Proximate Eclipse Trajectories (PETs) and are used to make hindsight and predictive analysis of the precipitation occurrences and magnitudes of given wet and dry spells. A remarkable accuracy of predictive capability was observed using PETs. For instance, in hindsight, the water year 2009 dry spell and 2010 wet spell in Northern California could have been predicted with 82% and 99% accuracy, respectively. Furthermore, similar storm event patterns and magnitudes were observed during two years that are in the same Saros series. Even though the extension of this analysis to global scale remains to be undertaken, the established SETs may well serve as the seeds for the formulation of guiding markers of hydrological conditions on earth.

Data Sources and Analysis

Historical and projected Solar and Lunar Eclipse data for the 1901 to 2100 period are available from NASA's Eclipse website (NASA, 2010). For this analysis, the historical solar eclipse data from 1901 through 2010 was used. The daily precipitation data at Davis since 1931 was obtained from the National Oceanic and Atmospheric Administration's (NOAA) National Climate Data Center (NCDC) (NOAA, 2010), through the California State Climatologist's Office. Daily data for earlier period was obtained from Utah State University's Climate Center (Utah State University, 2010). Monthly precipitation data for this location is available from the California Department of Water Resources Data Exchange Center (CDEC) (CA DWR, 2010).

NASA's data of historical solar eclipses shows that between 1901 and January of 2010, there were 81 Annular (A), 78 Total (T), and 7 Hybrid (H) solar eclipses. These eclipses are fairly uniformly distributed over the months of the years (see Table 1).

Table 1. Number of all (Annular, Total, and Hybrid) solar eclipses (SE) between 1901 and 2010

Month	Jan	Feb	Mar	Apr	May	Jun	Jul	Aug	Sep	Oct	Nov	Dec	Types of eclipses		
													Annular	Total	Hybrid
No. SE	16	15	15	13	13	15	14	15	12	14	12	12	81	78	7

A closer examination of these solar eclipse events shows distinguishable SET patterns. Similar patterns that are closely associated with established SETs are termed herein as Proximate Eclipse Trajectories (PETs). The occurrences or absences of solar eclipse

events during four seasons over a total of two water years were chosen to establish the seeds of specific SETs for the entire historical period during which solar eclipse data is available. For the purpose of this work, the October to March rainy season and April to September dry season in California are taken as the two seasons of the water year. A water year runs from the beginning of October of the previous calendar year to the end of September of the current calendar year. This characterization of a water year was recommended by Loewe and Radok (1948) to avoid splitting the Southern Hemisphere summer wet season, or equivalently, the Northern Hemisphere winter wet season.

While the relative positions of the earth, moon, and sun during the current water year's wet season is the primary focus to analyze how it affects hydrological conditions on earth during the same season, the two prior and one posterior seasons are included in SETs to trace the inertial state of the alignment before and after its realization. More emphasis is put on the priori state to inform the approaching inertial state to the realization during the current state. Thus, the four seasons of a SET as used herein are the current, the previous two, and the next seasons. These four seasons, which are subjectively limited, can be extended either into the past or future or both ways to obtain a more complete trajectory and their periodicities, a subject of further investigation. The three solar eclipse types, Annular, Total, and Hybrid, are designated herein with letter coding of A, T, and H, respectively. The season in which a solar eclipse happened is designated by the number of the month, with 1 for January, 2 for February, …, and 12 for December. Therefore, an A1 denotes an Annular solar eclipse in January. An A4-T10-A3-T9 SET denotes a trajectory of Annular eclipses in April of last year and March of the current year and Total eclipses in October of last year and September of the current year. The season in which no solar eclipse was observed is designated as NN. Thus, an NN-NN-NN-A4, which is the SET obtained for the 1976 record dry spell in California, denotes a period in which no solar eclipses occurred in both the current and previous years except one Annular eclipse in April of 1976.

Transient Spatial and Temporal Positions of the Earth and Moon around the Sun

To demonstrate the skills of the transient positions of the earth and moon around the sun in predicting wet and dry spells in California, Figure 1 attempts to illustrate a two dimensional vector field of these celestial objects. As shown in Table 1 and Figure 1, solar eclipse events can occur in any one of the twelve months of the year in one of several Saros series. Using the Saros cycles, solar eclipses have been organized into

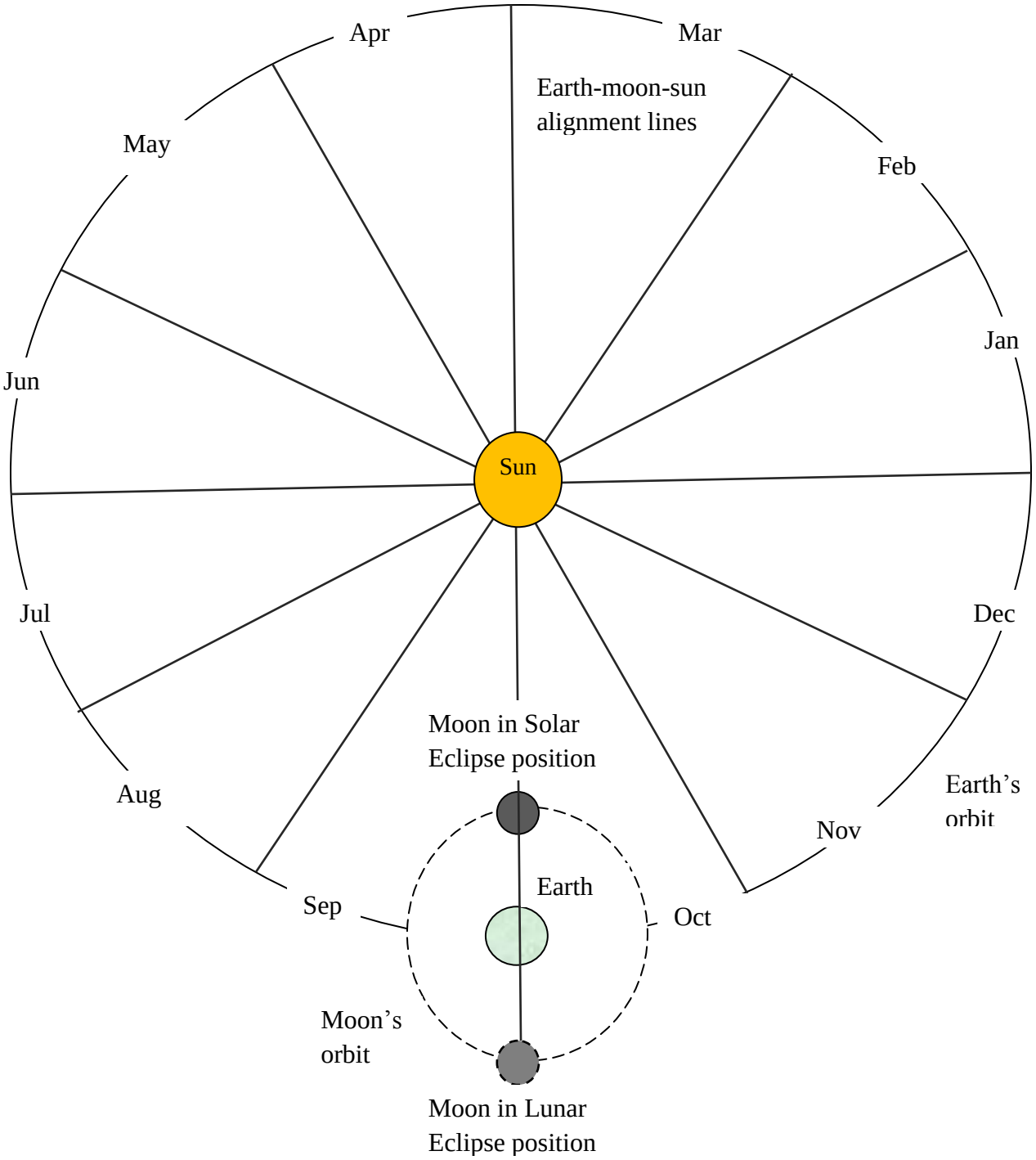

Figure 1. Schematic 2-dimensional (2D) rendering of the earth-moon-sun vector space and trajectories (not to scale)

families or series. According to NASA (2010), the Saros cycle, which is a period of 6585.3 days (18 years, 11 days, and 8 hours), governs the periodicities and recurrence of solar eclipses. When two eclipses are separated by a period of one Saros cycle, they share a very similar geometry and occur at the same node with the moon at nearly the same distance from earth and at the same time of year (NASA, 2010). Figure 2 presents these Saros series for the 1900 to 2100 period.

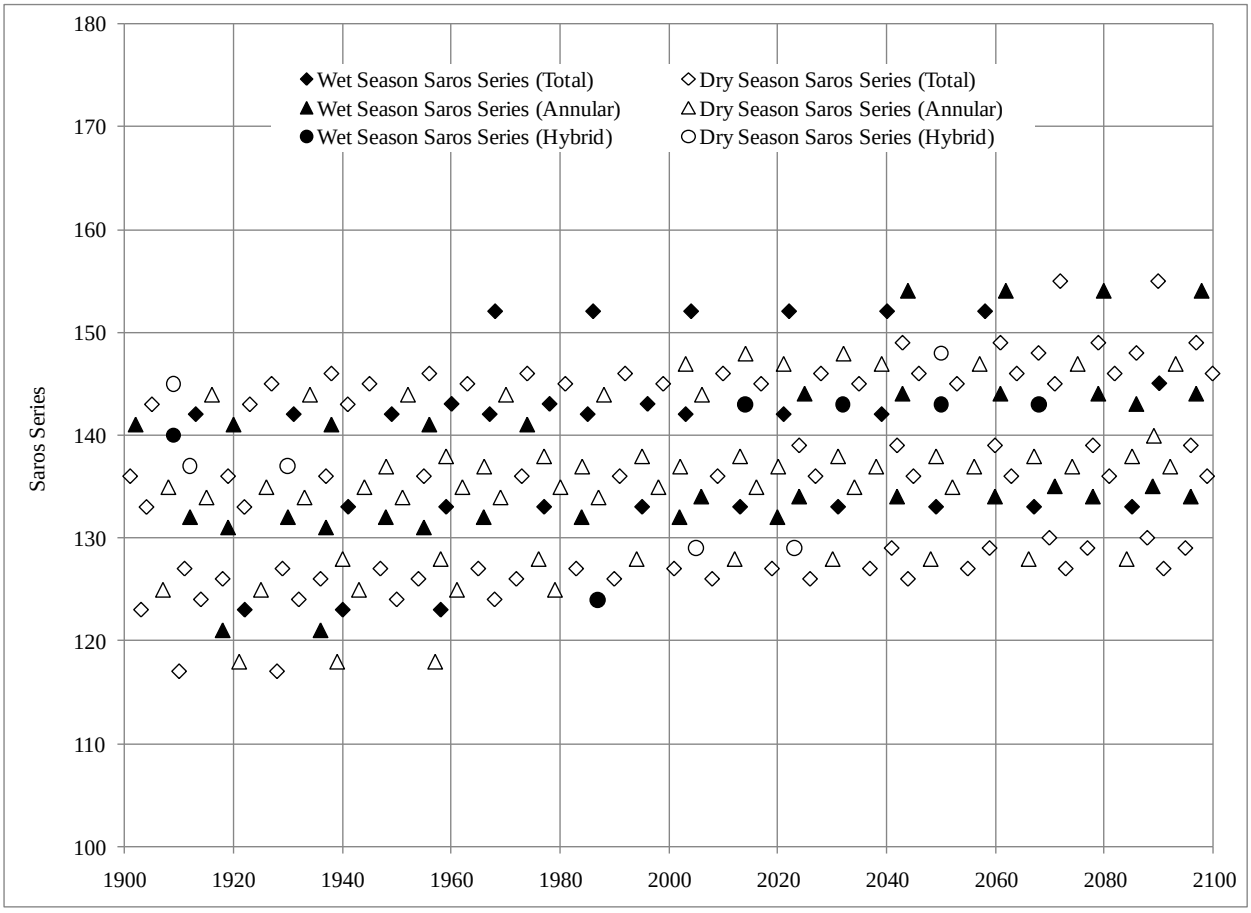

Figure 2. 20th and 21st century Saros series, which may be used for getting outlooks of hydrological conditions and variability on earth

Predicting Hydrological Conditions Using SETs

Using the established SETs discussed above, I categorized solar eclipse trajectories that may have similar geometry with the moon at nearly the same distance from the earth and at the same time of year. Figure 3 illustrates how these trajectories may be

determined for any given year. As an example, the specific trajectories for water years 1974, 1992, and 2010 have been drawn in Figure 3. The cumulative precipitation data of the wet season of these years are shown in Figure 4, which appears to display several phenomena. For instance, using the 1974 precipitation magnitude as the base, the precipitation during 1992 and 2010, two years that are in the same Saros series as 1974, are about 83% and 96%, a remarkable accuracy for prognostic value and implication. In some cases, a two-cycle Saros period tends to provide a better prediction than a single-cycle Saros period. In addition, the graphs for 1992 and 2010 appear to be nearly parallel. All the three graphs show a mix of periods with near horizontal and vertical slopes, possibly suggesting the effect of new and full moon phases on precipitation in addition to tidal dynamics. In fact, when the precipitation from the first storm in October of water year 2010 is removed, the 1992 and 2010 cumulative precipitation patterns and magnitudes are very similar.

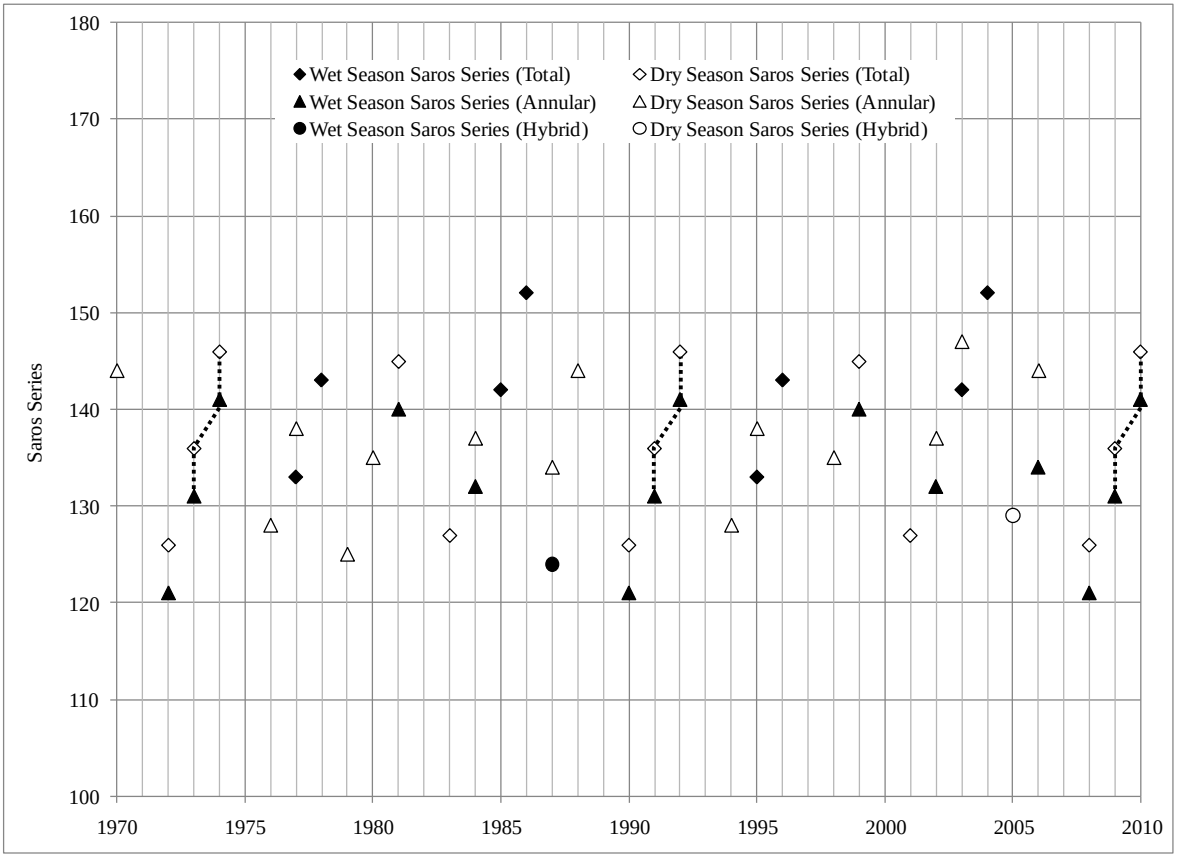

Figure 3. Solar eclipse trajectories for 1974, 1992, and 2010 (SET A1-T6-A12-T6, A1-T7-A1-T6, and A1-T7-A1-T7, respectively).

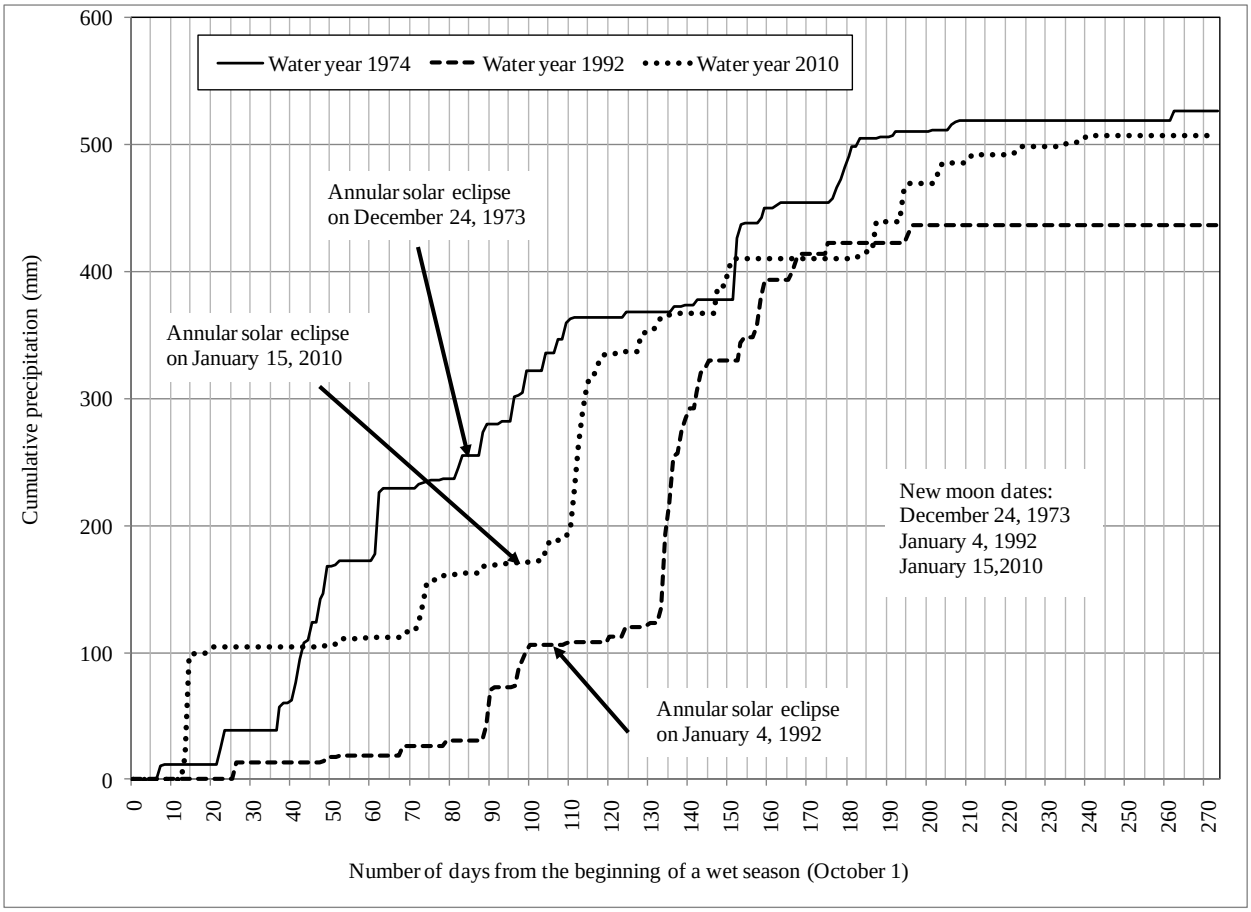

Figure 4. Cumulative precipitation magnitudes for the wet seasons of water years 1974, 1992, and 2010, which have similar SETs

Table 2 shows the precipitation magnitudes for fifteen pairs of water years that have clearly identifiable SETs for their similarities in each pair. The regression between the precipitation data of these identified groups of years shows a remarkable relationship with a coefficient of determination value of 0.94 (Figure 5). While these results are very interesting and appear to be promising for a decadal to multidecadal predictability of hydrological conditions on earth, more conclusive results may lie in the data of two years with identical positions of the moon during a period of identical times of the year. So far, what we have been able to observe are proximities, not identical ones.

Table 2. Historical precipitation data at Davis, California, for identified pairs of water years with similar Saros series and SETs

Identified pairs of years with similar Saros series and SETs	Precipitation during first year in the pair (mm)	Precipitation during second year in the pair (mm)	Percent difference with first year's precipitation as the base (%)
(1918, 1954)	337	345	2%
(1919, 1955)	404	382	-5%
(1928, 2001)	375	378	1%
(1929, 1947)	275	318	16%
(1930, 1948)	374	367	-2%
(1937, 1955)	373	382	2%
(1939, 1976)	180	173	-4%
(1944, 1962)	394	381	-3%
(1952, 1970)	526	433	-18%
(1955, 1991)	382	358	-6%
(1957, 1994)	310	302	-2%
(1970, 1988)	433	414	-4%
(1974, 2010)	542	523	-4%
(1978, 1996)	686	622	-9%
(1981, 1999)	311	268	-14%
Average difference			-5%

Discussion

The demonstration of multidecadal predictability of hydrological conditions on earth using Saros series, cycles, and SETs has, in many aspects, enormous implications for trainers, practitioners, and decision makers. As far removed from the earth as they seem to appear, the trajectories of the alignment of the moon and the sun relative to the earth have revealed yet another footprint in the hydrology on earth. No doubt that this study needs to be expanded to a global scale to ascertain that the relationships between SETs and hydrologic conditions on earth as evaluated using precipitation data at Davis, are reproducible in other parts of the world.

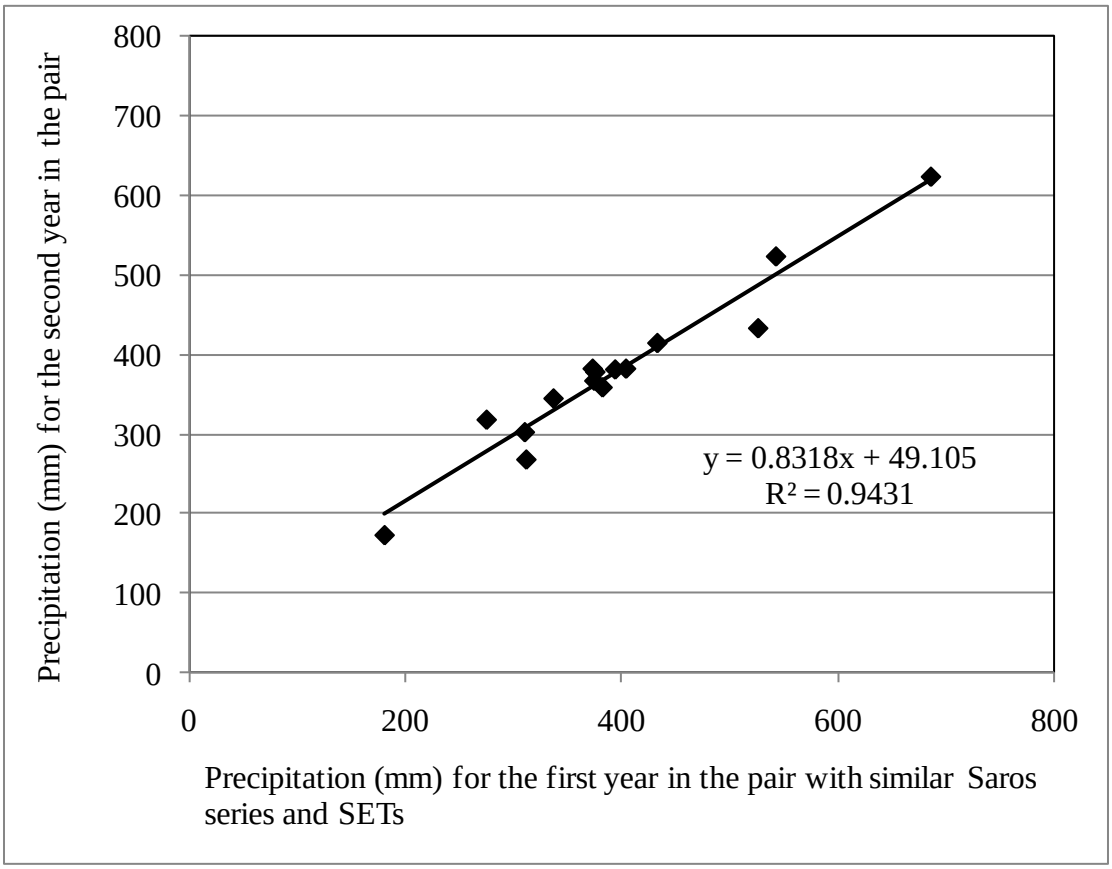

Figure 5. A regression between the historical precipitation data at Davis, California, for identified pairs of water years with similar Saros series and SETs

By creating a vector field in the sun-moon-earth space and the characterization of earth's hydrology in relation to the relative positions of these celestial objects in this vector field, we may be able to bring the predictability of wet and dry spells as well as non-extreme hydrological conditions on earth on a multidecadal scale within reach. Towards this end, SETs may be seen as nature's equivalents of DNAs and the earth system may be modeled as an animate matter that has its own periodic pulses. While this discovery does not directly address the issue of climate change, it is likely to go a long way in reducing the uncertainties surrounding the processes of general circulation modeling, which applies the law of thermodynamics to the earth system in isolation from the universe it is found in except using solar radiative forcing as a boundary condition.

References

CA DWR (2010), California Data Exchange Center, http://cdec.water.ca.gov/, accessed 01/22/2010

Goldenberg, S. B., C. W. Landsea, A. M. Mestas-Nuñez, and W. M. Gray (2001), The Recent Increase in Atlantic Hurricane Activity: Causes and Implications, *Science*, 293:5529, 474-479

Hurrell, J. W., Y. Kushnir., G. Ottersen, and M. Visbeck, M. (2003), In *North Atlantic Oscillation: Climate Significance and Environmental Impact*, Eds. Hurrell, J. W., Kushnir, Y., Ottersen, G. and Visbeck, M., Geophysical Monograph, 134, 1–35

Lettenmaier, D. P. and J. S. Famiglietti (2006), Water from on high, *Nature*, 444(30)

Loewe, F. and Radok, U. (1948), Variability and periodicity of meteorological elements in the Southern Hemisphere with particular reference to Australia, Canberra, Commonwealth of Australia

Madden, R. A. and P. R. Julian (1994), Observations of the 40–50 day tropical oscillation. *Monthly Weather Review,* 112, 1109–1123

Mantua, N. J. and S. R. Hare (2002) Journal of Oceanography, 58**,** 35–44

McCabe, G. J., M. A. Palecki, J. L. Betancourt (2004), Pacific and Atlantic Ocean influences on multidecadal drought frequency in the United States, PNAS 101, 4136-4141

Meehl, G. A., L. Goddard, J. Murphy, R. J. Stouffer, G. Boer, G. Danabasoglu, K. Dixon, M. A. Giogretta, A. M. Greene, E. Hawkins, G. Hegerl, D. Karoly, N. Keenlyside, M. Kimoto, B. Kirtman, A. Navarra, R. Pulwarty, D. Smith, D. Stammer, and T. Stockdale, Decadal prediction: can it be skillful?, American Meteorological Society, 1467-1485

Milly, P. C. D., J. Betancourt, M. Falkenmark, R. M. Hirsch, Z. W. Kundzewicz, D. P. Lettenmaier, R. J. Stouffer (2008), Stationarity is dead: wither water management?, Science 319, 573-574

NASA (2010), NASA Eclipse Web Site, http://eclipse.gsfc.nasa.gov/eclipse.html, accessed 01/22/2010

NOAA (2010), National Climate Data Center, http://www.ncdc.noaa.gov/oa/ncdc.html, accessed 01/21/2010

Office of the Governor (2009), Gov. Schwarzenegger Takes Action to Address California's Water Shortage, http://gov.ca.gov/press-release/11556/ (accessed December 27, 2009)

Rahmstorf, S. (2002), Ocean circulation and climate during the past 120,000 years, Nature, 419, 207-214

Trenberth, K. and D. J. Shea (1987), On the evolution of the Southern Oscillation, *Monthly Weather Review,* **115**, 3078–3096

Utah State University (2010), Utah Climate Center, http://climate.usurf.usu.edu/products/data.php (accessed October 17, 2010)

Willett, H. (1974), Recent Statistical Evidence in Support of the Predictive Significance of Solar-Climatic Cycles, *Monthly Weather Review*, 102: 679-686

Wood, F. J. (2001), Tidal Dynamics, Volume I: Theory and Analysis of Tidal Forces, *Journal of Coastal Research (JCR) Special Issue No. 30*, Coastal Education and Research Foundation (CERF), West Palm Beach, Fla.

Wu, Z., B. Wang, J. Li, and F.-F. Jin (2009), An empirical seasonal prediction model of the east Asian summer monsoon using ENSO and NAO, J. Geophys. Res., 114

Astrohydrology and the Predictability of Hydrological Variability[1]

Messele Zewdie Ejeta

Abstract

This paper presents the uncovering of a new evidence that when the earth and moon are at nearly the same distance from the sun at the same time of year, similar hydrological conditions are observed across the United States, as tested using the long term historical precipitation data of a cross-section of gauging stations. The Saros cycle and recorded solar eclipse trajectories are used as measures for these celestial objects' relative astronomical positions. The analysis results show that these measures provide high prognostic skills that can be of practical significance in multidecadal prediction of hydrological variability in the U. S. and most likely on a global scale. This finding may be poised to lead us to a better planning for and management of water stresses, excesses, and transfers. In effect, it is likely to point to a deterministic solution of the paradoxical hydrological stationarity problem, the reduction of uncertainties in climate change modeling, and the opening of a new specialty area for hydrology, which may be termed Astrohydrology – the study of hydrology using astronomical observations.

Introduction

The prognostication of hydrological variability on a multidecadal scale, a longtime challenge hitherto, has enormous importance in the planning and management of natural resources, including water. The general idea of hydrological stationarity, which holds that natural systems fluctuate within an unchanging envelope of variability, has been intuitively established for practical purposes. In general, humanity has often relied on the mercy of nature in its management and utilization of natural resources. It has also been continuously knocking at the doors of nature to better understand the fundamental processes behind it. Major successes have been achieved and many continue to be pursued. Closing the earth's water balance has been the dream of hydrologists for long (Lettenmaier and Famiglietti, 2006). The prediction of hydrological conditions on the earth on a decadal to multidecadal scale is one of such efforts that have been daunting. Its success could lead to, among others, better managements of floods, droughts, and economical water transfers.

[1] This article was submitted on August 19, 2010, to the Journal of Hydrology for review and possible publication. A letter of rejection was received on February 10, 2011.

Projected climate change studies rely on general circulation modeling approaches that inherently embody the uncertainty about the underlying fundamental processes that have made nature, as well as the earth's natural hydrological variability, as it has been while attempting to provide a projected state that it could exhibit because of elevated Green House Gas (GHG) concentration in the atmosphere. One of the interesting aspects in the efforts to use the results of general circulation modeling is the treatment of hydrological data using statistical metrics. Utilizing the statistical characteristics of hydrological data involving the results of general circulation modeling includes 1) disaggregating global scale general circulation model results to local scale hydrological data (Wood, et al., 2004, Wood et al., 2002), 2) using the statistical measures of observed hydrological data in comparing and using disaggregated hydrological data in macro scale hydrological models (Maurer, et al., 2010), and 3) the assessment of the impact of climate change on water projects (Chung, et al, 2010, Anderson, et al., 2007, Christensen, et al., 2007). The basic impediment to using dynamical modeling instead of statistical metrics in utilizing the results of general circulation model results is cited to be the computational requirement of the former (Maurer, et al., 2010). To the extent that: 1) general circulation modeling relies on the application of the second law of thermodynamics to the earth and its atmospheric boundary in isolation from this celestial object's possible natural interactions with other celestial objects, and 2) there exists conflicting signals between deterministic and stochastic natures of the earth's natural hydrological variability, our efforts at the assessment of the impact of climate change on complex projects and the utilization of such assessments for decision making purposes are likely to come with significant caveats. While a stochastic hydrological variability on the earth has been presumed and utilized for various planning purposes, its deterministic nature has been implicitly stated by Milly, et al. (2008) and explicitly formulated by Ejeta (2010, under review), which is also shown below.

The current work provides more evidences for the deterministic nature of hydrological conditions on the earth by presenting the analysis results of long term precipitation records at a cross-section of gauging stations in the U. S. These results show that hydrological conditions on the earth can be predicted on a decadal to multidecadal scale through the study of the positions of the earth and moon from the sun and the time of the year, as inferred from Saros cycle and solar eclipse trajectories, both of which have projected data from NASA (2010) out to the end of this century.

The Hydrological Stationarity Problem

Let P_1, P_2, P_3, …, P_N be the water year precipitation records of N years at a given gauging station where $N \geq 30$. We can define the average precipitation of the gauging station using a simple arithmetic mean formulation given by Equation 1.

$$\bar{P} = \frac{\sum_{i=1}^{N} P_i}{N} \quad (1)$$

where $\bar{P}$ is the average precipitation at the gauging station and i stands for an individual year in a set of N years.

For any n consecutive water years that are a subset of N water years, the paradoxical stationarity problem can be formulated as given by Equation 2. According to the World Meteorological Organization (WMO), a period of 30 years represents a climatological standard normal, which is defined as the average of climatological data computed for the following consecutive periods of 30 years (WMO, 1988).

$$\bar{P} = \frac{\sum_{i=1}^{n} P_i}{n} - \varepsilon_1 = \frac{\sum_{i=2}^{n+1} P_i}{n} - \varepsilon_2 = \frac{\sum_{i=3}^{n+2} P_i}{n} - \varepsilon_3 = \cdots = \frac{\sum_{i=(N-n+1)}^{N} P_i}{n} - \varepsilon_{(N-n+1)} \quad (2)$$

where $\varepsilon_1, \varepsilon_2, \varepsilon_3, \ldots \varepsilon_{(N-n+1)}$ are residual departures from stationarity. For practically insignificant residuals, as was observed in recorded long term precipitation data of the three gauging stations in northern California, namely Red Bluff, Davis, and Napa, Equation 2 may be rewritten as Equation 3.

$$\bar{P} \approx \frac{\sum_{i=1}^{n} P_i}{n} \approx \frac{\sum_{i=2}^{n+1} P_i}{n} \approx \frac{\sum_{i=3}^{n+2} P_i}{n} \approx \cdots \approx \frac{\sum_{i=(N-n+1)}^{N} P_i}{n} \quad (3)$$

Equation 3, which is hereafter called the Hydrological Stationarity Problem, is likely to point to a composite of deterministic harmonic functions, which can be decomposed into unique pseudo sinusoidal functions that have their own periodicities, a subject of continuous investigation.

Methodology

In order to show the skills of the relative positions of the earth and moon from the sun at the same time of the year in the prediction of natural hydrological variability across the U. S., this study first attempts to create a vector field in the earth, moon, and sun space (Figure 1) and then analyzes the hydrological conditions in the U.S. Historical solar eclipse characteristics and trajectories are used to determine proximities for when the earth and moon are at nearly the same distance from the sun

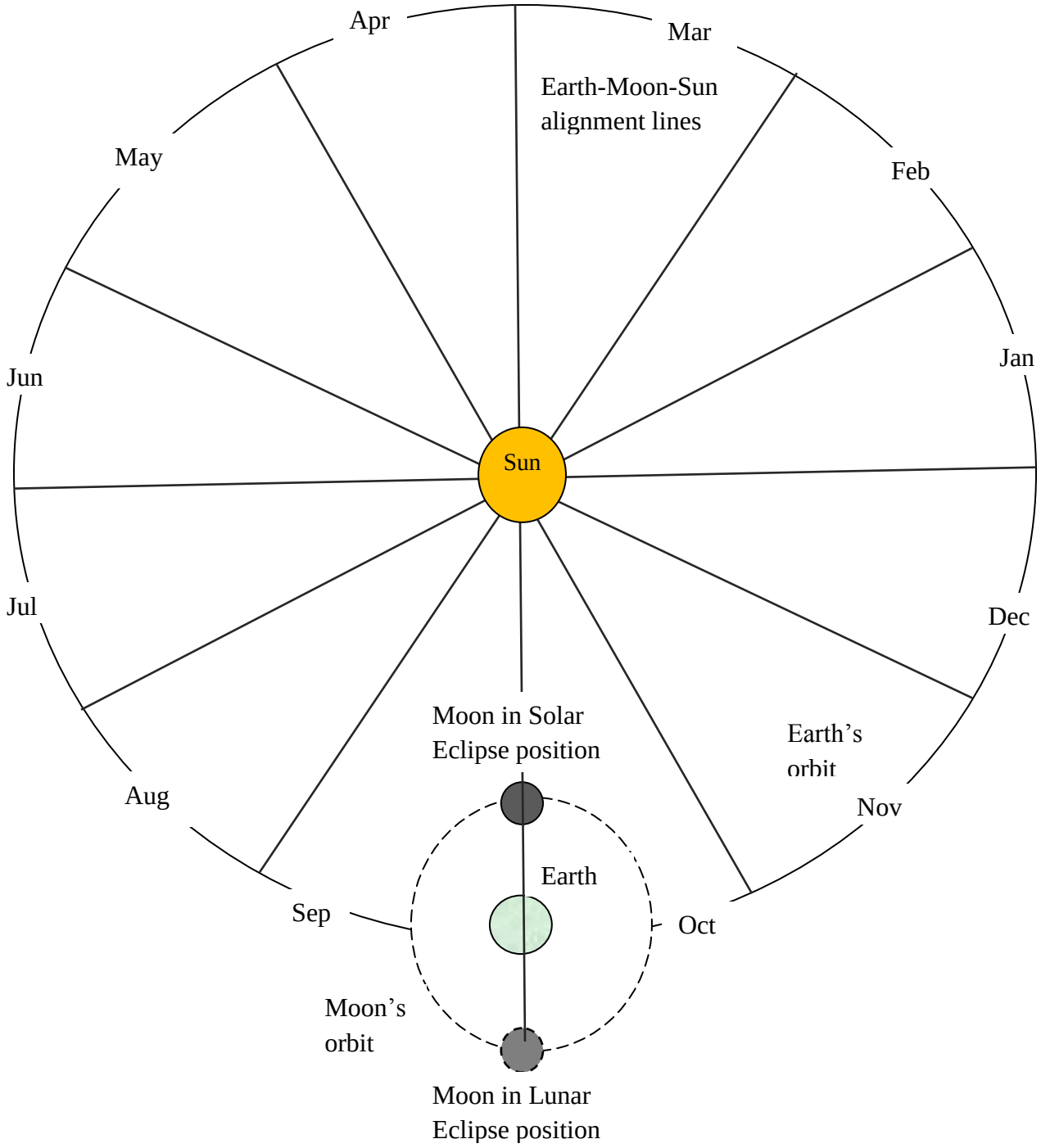

Figure 1. Schematic 2-dimensional (2D) rendering of the Earth-Moon-Sun vector space and trajectories (not to scale)

at the same time of year. A four season, or two water year, time window is used in identifying proximate solar eclipse trajectories. While the main objective in defining and characterizing these solar eclipse trajectories is to determine the relative position of the earth and moon from the sun during the current water year as well as the timing of the proximate relative astronomical positions of these celestial objects, the previous water year's relative positions of these objects are also considered to get an understanding of the precedent state to the current water year's state. A water year runs from the beginning of October of the previous calendar year to the end of September of the current calendar year. This characterization of a water year was recommended by Loewe and Radok (1948) to avoid splitting the Southern Hemisphere summer wet season, or equivalently, the northern Hemisphere winter wet season. For the purposes of this analysis, a water year is split between the October to March wet season and April to September dry season.

Solar eclipse events have been characterized by NASA (2010) as Total (T), Annular (A), and Hybrid (H). I define a solar eclipse trajectory using these letter notations to represent the characteristics of the eclipse event along with the calendar month's number in which it occurred. Therefore, an A4 denotes an annular solar eclipse event that occurred in April. As indicated earlier, to define a solar eclipse trajectory of the current water year, I extend this definition to the previous and current water years and characterize its evolving solar eclipse trajectory. An absence of a solar eclipse event during any season is denoted by NN. Thus, an A12-T5-NN-A4 denotes a solar eclipse trajectory with an Annular solar eclipse event in December of the previous water year, Total solar eclipse event in May of the previous water year, no solar eclipse event in the first half of the current water year, and an Annular solar eclipse in April of the current water year. This notation provides unique identifications of solar eclipse trajectories for a time window of any two water years.

Some solar eclipse trajectories are similar in occurrence due to the cyclic nature of the characteristics and timing of these events. A study of the developed pool of solar eclipse trajectories for a time window of two years shows that two years that are one Saros cycle (NASA, 2010) apart show similar characteristics. For instance, water years 1939 and 1957 have, according to the characterization herein, solar eclipse trajectories of A12-T5-NN-A4 and A12-T6-NN-A4, respectively. The A12-T5-NN-A4 trajectory for water year 1939 shows that there was an Annual solar eclipse event in December 1937 (water year 1938), a Total solar eclipse event in May 1938, no solar eclipse in the first half of water year 1939, and an Annular solar eclipse event in April 1939. The A12-T6-NN-A4 trajectory for water year 1957 is similar to that of water year 1939 except the Total eclipse in its trajectory occurred in June (6/8/1956), instead of May

(5/29/1938), which was the case for the trajectory of water year 1939. On the basis of these similarities in the relative positions of these celestial objects at the same time of year, the datasets of two different pairs of years that are one Saros cycle (NASA, 2010) apart were analyzed. Each set of years is used to show the predictability of dry and wet conditions using these relative positions and time of year.

Results

Table 1 presents similar solar eclipse trajectories for which long term data of a cross section of gauging stations across the U.S. was analyzed for dry hydrological conditions. Similarly, Table 2 presents the equivalent solar eclipse trajectories for which the data was analyzed for wet hydrological conditions. A list of the gauging stations used is presented in Table 3 along with the geographic location characteristics of these stations.

Each set of the solar eclipse trajectories presented in both Table 1 and Table 2 were screened based on their similar nature to the other trajectories in their respective sets. The trajectories for the dry conditions in Table 1 are characterized by the lack of solar eclipse events in the first half of the current water year and an Annular solar eclipse event in April or May of the second half of the water year. On the other hand, the trajectories for the wet conditions in Table 2 are characterized by an Annular solar eclipse event in January or February of the current water year followed by a Total solar eclipse event during the June to August season of the second half of the water year. Note that the eclipse trajectories in each table are one Saros cycle apart from the previous or subsequent similar eclipse trajectory.

Table 1. Selected solar eclipse trajectories with similar eclipse characteristics, which were found to correspond to dry hydrological conditions in northern California since the early 20th century

Water Year	Solar eclipse trajectory*	Solar eclipse dates	Saros series	Gamma	Eclipse magnitude	Path width (Km)
1921	A11-NN-NN-**A4**	11/22/1919, none, none, **4/8/1921**	**118**	**0.8869**	**0.975**	**191.5**
1939	A12-T5-NN-**A4**	12/2/1937, 5/29/1938, none, **4/19/1939**	**118**	**0.9388**	**0.973**	**285.0**
1957	A12-T6-NN-**A4**	12/14/1955, 6/8/1956, none, **4/30/1957**	**118**	**0.9992**	**0.980**	**N/A**
1976	NN-NN-NN-**A4**	None, none, none, **4/29/1976**	**128**	**0.3378**	**0.942**	**227.4**
1994	NN-NN-NN-**A5**	None, none, none, **5/10/1994**	**128**	**0.4077**	**0.943**	**230.1**
2012	NN-NN-NN-**A5**	None, none, none, **5/20/2012**	**128**	**0.4828**	**0.944**	**236.9**

* The solar eclipse characteristics of Saros series, Gamma, eclipse magnitude, and path width (km) are for those events indicated in bold in the notations of the trajectories

Table 2. Selected solar eclipse trajectories with similar eclipse characteristics, which were found to correspond to wet hydrological conditions in northern California since the early 20th century

Water Year	Solar eclipse trajectory*	Solar eclipse dates	Saros series	Gamma	Eclipse magnitude	Path width (Km)
1927	T1-A7-**A1**-T6	1/14/1926, 7/9/1926, 1/3/1927, 6/29/1927	**140**	**-0.4956**	**0.999**	**2.1**
1945	T1-A7-**A1**-T7	1/25/1944, 7/20/1944, 1/14/1945, 7/9/1945	**140**	**-0.4937**	**0.997**	**11.9**
1963	T2-A7-**A1**-T7	2/5/1962, 7/31/1962, 1/25/1963, 7/20/1963	**140**	**-0.4898**	**0.995**	**19.7**
1981	T2-A8-**A2**-T7	2/16/1980, 8/10/1980, 2/4/1981, 7/31/1981	**140**	**-0.4838**	**0.994**	**25.0**
1999	T2-A8-**A2**-T8	2/26/1998, 8/22/1998, 2/16/1999, 8/11/1999	**140**	**-0.4726**	**0.993**	**28.8**

* The solar eclipse characteristics are for those events indicated in bold in the trajectories

Table 3. A cross section of gauging stations across the U. S. used for the analysis

No.	Precipitation gage station	Latitude	Longitude
1	Indian Mills, New Jersey	39.8144	-74.7883
2	Cooperstown, New York	42.7167	-74.9267
3	Ithaca, New York	42.4489	-76.4489
4	Winchester, Virginia	39.1833	-78.1167
5	Knoxville, Tennessee	35.8181	-83.9858
6	Atlanta Hartsfield Airport, Georgia	33.6300	-84.4417
7	Selma, Alabama	32.4100	-87.0153
8	Charleston, Illinois	39.4761	-88.1653
9	Black Rock, Arkansas	36.1067	-91.1039
10	Farmington, Minnesota	44.6697	-93.1700
11	Purcell, Oklahoma	35.0325	-97.3733
12	Bridgeport, Texas	33.2064	-97.7761
13	Fort Collins, Colorado	40.6147	-105.1310
14	Mesa, Arizona	33.4114	-111.8180
15	Salt Lake City Airport, Utah	40.7781	-111.9690
16	Medford International Airport, Oregon	42.3811	-122.872

The analysis of recorded precipitation data of the cross-section of gauging stations in the U. S. that are listed in Table 3 shows that the hydrological conditions at these gauging stations, as measured by the recorded precipitation magnitude, embody an important level of predictive skill, as demonstrated in hindsight. The results show that the dry conditions of 1939, 1957, 1976, and 1994, all of which have similar solar eclipse trajectories (**-**-NN-A4) for their respective current water years, exhibit

comparable precipitation magnitudes at these gauging stations. Similarly, the wet conditions of 1945, 1963, 1981, and 1999, all of which have similar solar eclipse trajectories (**-**-A1/A2-T6/T7/T8) for their respective current water years, exhibit comparable precipitation magnitudes. Two sample results, one for dry conditions and another for wet conditions, are shown in Figure 2 and Figure 3. The result in Figure 2 shows that the dry condition in water year 1976 could have been explained, on average, with a coefficient of determination of approximately 73% using water year 1939's solar eclipse trajectory and precipitation data. Similarly, the result in Figure 3 shows that the wet condition in water year 1999 could have been explained, on average, with a coefficient of determination of approximately 59% using water year 1963's solar eclipse trajectory and precipitation data.

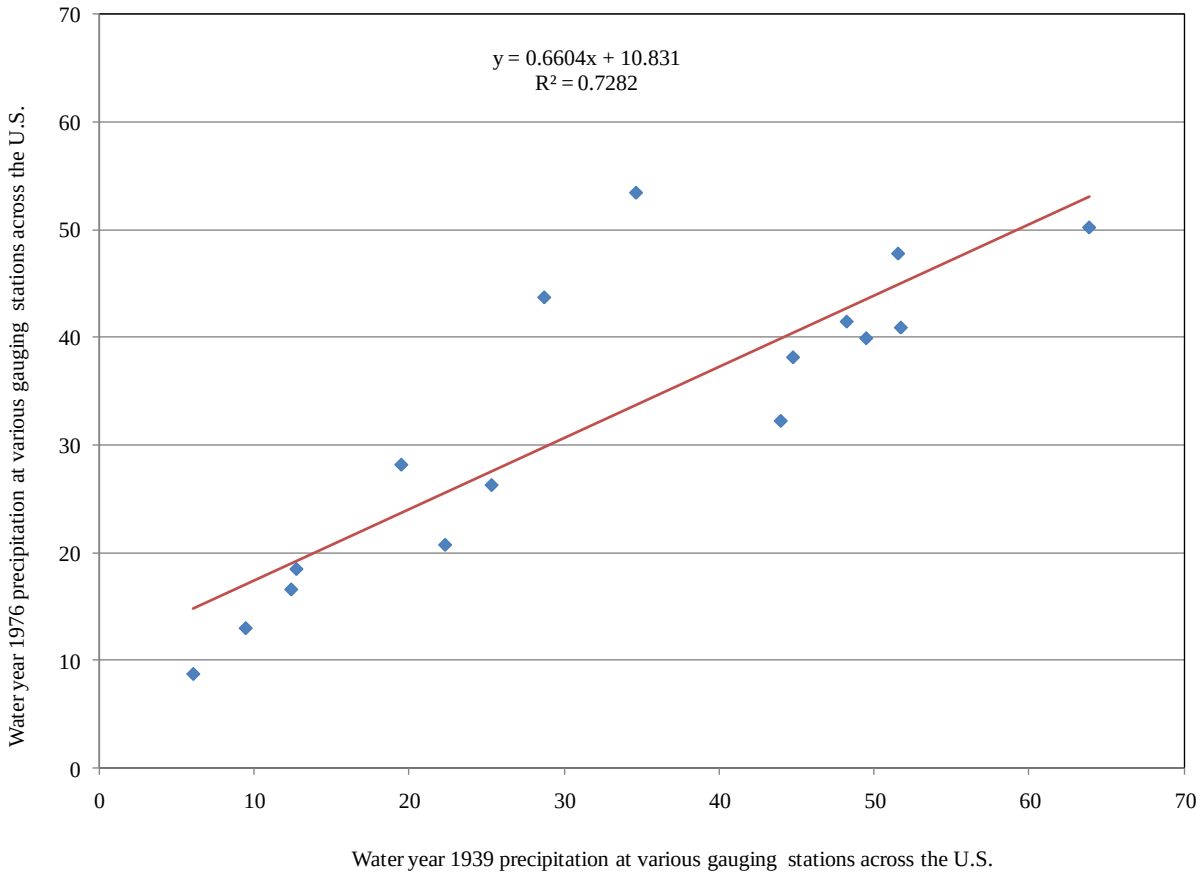

Figure 2. This chart illustrates how water year 1939 and 1976 precipitation data across gauging stations in the U. S. compare to each other. Both water years have similar solar eclipse trajectories, A12-NN-NN-A4 and NN-NN-NN-A4, respectively.

Based on the above analyses and available projected solar eclipse trajectories from NASA (2010) for this century, water year 2012 is the next nearly similar water year type to those that have coincided with dry conditions in northern California during the last century. Accordingly, water year 2012 is likely to exhibit similar hydrological conditions as 1994. However, more rigorous local to global scale verifications, a subject of an ongoing investigation, are needed before such findings can be used for decision making purposes.

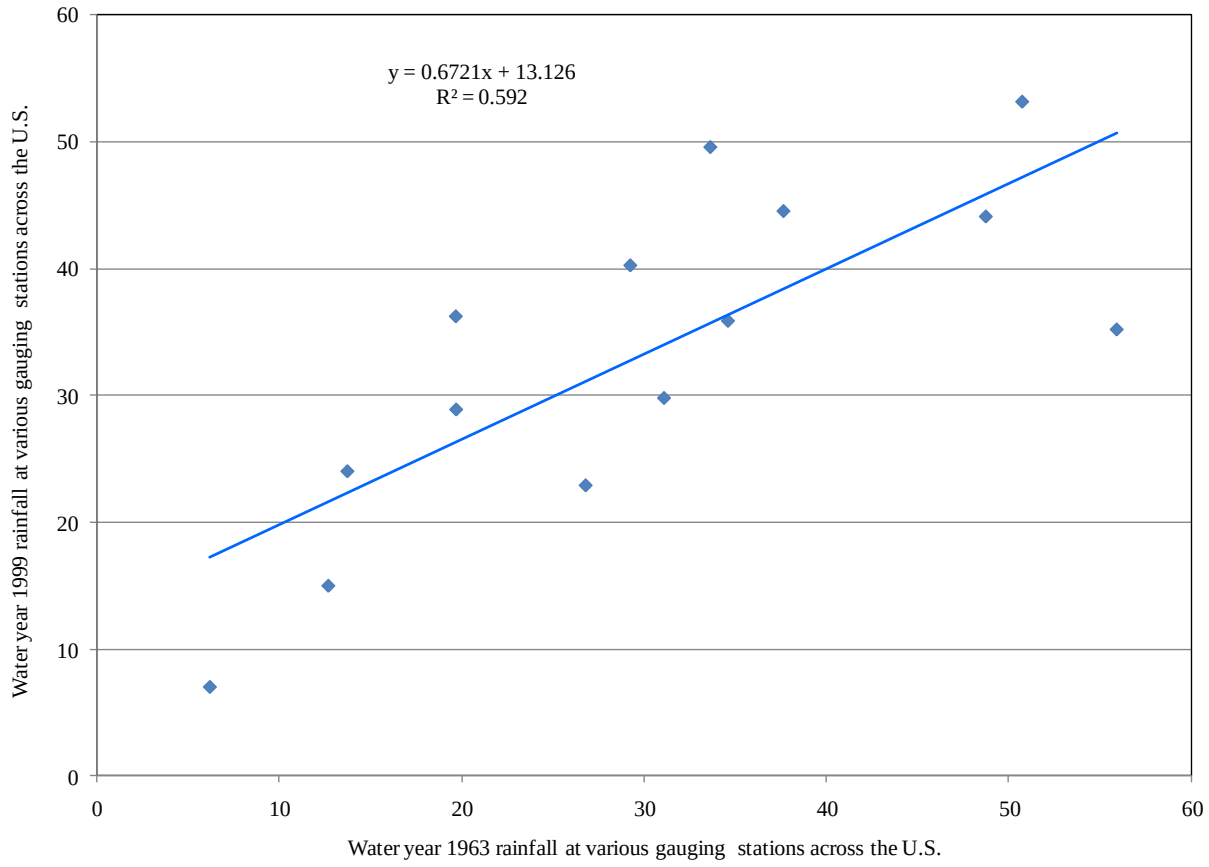

Figure 3. This chart illustrates how water year 1963 and 1999 precipitation data across gauging stations in the U. S. compare to each other. Both water years have similar solar eclipse trajectories, T2-A7-A1-T7 and T2-A8-A2-T8, respectively.

Discussion

The nature of Equation 3 appears to be inherently deterministic. This conceptual premise is supported by the stationary nature of the precipitation data at the three

northern California locations. A study of over a century of the precipitation data of these locations shows that the average departure from the long term average for any given climatological period of 30 years is less than 1% for each of the locations. In addition, the maximum and minimum climatological period departures are less than 3% in magnitude for each of these locations. This suggests that the 30-year climatic period average water supply from precipitation for each of these locations could have been predicted with over 97% precision starting any year since the early 20th century. The paradox of hydrological stationarity has been stated thus as follows: If the natural water supply from precipitation for a given location for the next thirty years, starting any year in the last century, could be predicted with this high level of precision, why can't the water production of the same watershed for the subsequent 5 or 10 years be predicted with the same or higher level of precision? (Ejeta, under review). The analysis presented in the current work suggests that two years that are characterized by similar relative astronomical positions of the earth, moon, and sun at the same time of the year have similar hydrological conditions on the earth.

This prevalence of similar hydrological conditions across the U. S. for similar relative astronomical positions of these celestial objects at the same time of year has been shown through the analysis of recorded long term precipitation data of a cross section of its gauging stations. This finding points to a shift from a stochastic analysis of hydrological variability to its deterministic prognostication well into the future. To the extent that there exists a relationship between the positions of the earth, moon, and sun in the Earth-Moon-Sun vector space and natural hydrological variability in the U. S., it is presumed that this relationship is most likely to be at play on a global scale. These presumption needs verification, which is a subject of an ongoing investigation. Even though this initial finding needs consolidation through further analysis of observed data on a global scale, this continental scale finding has enormous implications for water resources planning purposes. The ability to prognosticate natural hydrological variability well into the future has enormous importance in the management of water stresses (droughts) and excesses (floods) as well as in the economic considerations of water transfers.

This finding may also be bound to reduce the uncertainty surrounding climate change modeling processes. A meaningful handle on the natural variability of climate, as reflected in the earth's natural precipitation variability, is likely to help isolate the incremental effects of elevated GHG concentration in the atmosphere. This approach may be very useful in testing the performance of various General Circulation Models (GCMs) by reviewing how best they reproduce a characterized natural variability before tackling the incremental effects of elevated GHG concentration in the

atmosphere. Any model needs to provide meaningful results from the modeling of the state of the system as it is prior to providing sensible enough results from the modeling of the altered state of the system. Inasmuch as this premise in modeling is very important, this finding may help sort out GCMs in their importance of modeling the state of the system as it is and hence the altered state of the system as it is projected to become due to elevated GHG concentration in the atmosphere.

At a professional level, this finding is likely to create a new area of specialty, which may be termed Astrohydrology and defined as the study of the earth's hydrological variability in relation to astronomical observations. To the extent that the relative positions of the earth, moon, and sun have been characterized and can be characterized further in relation to the positions of other celestial objects, there may not be a time in the future when humanity will not have a meaningful prognostication of hydrological conditions on the earth. This appears to stand to suggest that future is a construction of our perception of the reality of a moment in the space, which is illustrated in Figure 1. This understanding my lend humanity to the resignation that, in some ways, what has occurred naturally is a precursor to what is to occur when the cyclic nature of the celestial objects in our solar system reposition themselves at the same moment in their vector space.

References

Anderson, J., F. Chung, M. Anderson, L. Brekke, D. Easton, M. Ejeta, R. Peterson, and R. Snyder (2007), Progress on incorporating climate change into management of California's water resources, Climatic Change, 91-108.

Christensen, N. S. and D. P. Lettenmaier (2007), A multimodel ensemble approach to assessment of climate change impacts on the hydrology and water resources of the Colorado River Basin, Hydrology and Earth System Sciences, 11, 1417-1434.

Chung, F., J. Anderson, S. Arora, M. Ejeta, J. Galef, T. Kadir, K. Kao, A. Olson, C. Quan, E. Reyes, M. Roos, S. Seneviratne, J. Wang, H. Yin (2010), An Iterative Approach for Assessing Climate Change Impacts, Journal of Water Resources Planning and Management, accepted.

Ejeta, M. Z. (in progress), The Paradox of Hydrological Stationarity: Towards a Deterministic Solution, Journal of Stationarity.

Lettenmaier, D. P. and J. S. Famiglietti (2006), Water from on high, *Nature*, 444(30).

Loewe, F. and Radok, U. (1948), Variability and periodicity of meteorological elements in the Southern Hemisphere with particular reference to Australia, Canberra, Commonwealth of Australia.

Maurer, E. P., H. G. Hidalgo, T. Das, M. D. Dettinger, and D. R. Cayan (2010), The utility of daily large-scale climate data in the assessment of climate change impacts on daily streamflow in California, Hydrology and Earth System Sciences, 14, 1125-1138.

Milly, P. C. D., J. Betancourt, M. Falkenmark, R. M. Hirsch, Z. W. Kundzewicz, D. P. Lettenmaier, R. J. Stouffer (2008), Stationarity is dead: wither water management?, Science 319, 573-574.

National Aeronautics and Space Administration (NASA) (2010), NASA Eclipse Website, http://eclipse.gsfc.nasa.gov/eclipse.html (last accessed July 16, 2010).

WMO (1988), General Meteorological Standards and Recommended Practices, Technical Regulations, Volume I, Basic Documents No. 2, WMO Publication No. 49, Geneva, Switzerland.

Wood, A. W., L. R. Leung, V. Sridhar, and D. P. Lettenmaier (2004), Hydrologic implications of dynamical and statistical approaches to downscaling climate model outputs, Climatic Change, 62, 189-216.

Wood, A. W., E. P. Maurer, A. Kumar, and D. P. Lettenmaier (2002), Long-range experimental hydrologic forecasting for the eastern United States, Journal of Geophysical Research, 107.